SCIENCE CHINA
Technological Sciences

·Special Topic· Optical Engineering
• Review •

December 2017 Vol.60 No.12:1801–1818
doi: 10.1007/s11431-017-9057-3

Optically pumped terahertz sources

ZHONG Kai[1,2], SHI Wei[1,2*], XU DeGang[1,2], LIU PengXiang[1,2], WANG YuYe[1,2], MEI JiaLin[1,2], YAN Chao[1,2], FU ShiJie[1,2] & YAO JianQuan[1,2]

[1]*Institute of Laser and Optoelectronics, College of Precision Instrument and Opto-electronics Engineering, Tianjin University, Tianjin 300072, China;*
[2]*Key Laboratory of Opto-electronics Information Technology (Ministry of Education), Tianjin University, Tianjin 300072, China*

Received February 19, 2017; accepted April 24, 2017; published online June 15, 2017

High-power terahertz (THz) generation in the frequency range of 0.1–10 THz has been a fast-developing research area ever since the beginning of the THz boom two decades ago, enabling new technological breakthroughs in spectroscopy, communication, imaging, etc. By using optical (laser) pumping methods with near- or mid-infrared (IR) lasers, flexible and practical THz sources covering the whole THz range can be realized to overcome the shortage of electronic THz sources and now they are playing important roles in THz science and technology. This paper overviews various optically pumped THz sources, including femtosecond laser based ultrafast broadband THz generation, monochromatic widely tunable THz generation, single-mode on-chip THz source from photomixing, and the traditional powerful THz gas lasers. Full descriptions from basic principles to the latest progress are presented and their advantages and disadvantages are discussed as well. It is expected that this review gives a comprehensive reference to researchers in this area and additionally helps newcomers to quickly gain understanding of optically pumped THz sources.

terahertz (THz) wave, photoconductive switch, optical rectification, difference frequency generation (DFG), terahertz parametric oscillator (TPO), photomixing, THz gas lasers, phase matching (PM)

Citation: Zhong K, Shi W, Xu D G, et al. Optically pumped terahertz sources. Sci China Tech Sci, 2017, 60: 1801–1818, doi: 10.1007/s11431-017-9057-3

1 Introduction

Terahertz (THz) waves, ranging from 100 GHz to 10 THz in frequency (3 mm to 30 μm in wavelength) between microwave and infrared (IR), used to be a "gap" in electromagnetic spectrum because the lack of efficient generating and detecting methods. However, this gap has now been filled, at least in part, with the scientific development and technological innovation since the end of the last century. Although not fully exploited, the rapidly growing THz technology is now pervading almost all the basic subjects including biology, physics, chemistry, material sciences, etc. [1–3]. THz outputs (number of documents with "terahertz" appearing in the abstract, title or keyword) have been growing exponentially in the past two decades [4]. The once anticipated "potential" applications, such as spectroscopy, medical imaging, radar, communication and non-destructive inspection, are also becoming practical facilities and creating big opportunities in the world market.

Nowadays, finding THz sources is still one of the obstacles restricting the development of applications for THz technologies. Although thermal sources like the mercury lamp and globar have been used as wide band THz sources in laboratory since long time ago, they are essentially long-wave IR sources and THz waves are merely a by-product, and the low brightness, incoherence and short lifetime restrict them to be used

*Corresponding author (email: shiwei@tju.edu.cn)

in simple applications like spectroscopy. Generally, there are two methods for THz wave generation—electronic and photonic [4–9]. The electronic method includes two types, in which back-ward wave oscillators, travelling-wave tubes, gyrotrons, and free-electron lasers are vacuum electronic devices, while Gunn diode, high-frequency transistors and frequency multipliers are solid-state electronic devices. Electronic THz sources dominate in the low-frequency part but most of them are unable to cover the high-frequency range above 1 THz. Photonic THz sources can also be divided into two categories, the so-called THz lasers and optical-to-THz conversion. THz lasers are built from the archetypical elemental semiconductors—germanium and silicon, or gases like CH_3OH, HCOOH and CH_2F_2. The solid-state semiconductor lasers, e.g. p-germanium laser and quantum cascaded lasers, are electrical pumped and being challenged by raising the operating temperature. THz gas lasers are pumped by IR lasers (e.g. CO_2 lasers around 10.6 μm) with the main disadvantage of showing bulky and discrete lines. The other photonic THz sources are all pumped by lasers and converted to THz, using the methods of nonlinear frequency conversion, photoconductive switches or antennas, etc.

Lasers have been playing important roles in THz generation. The trigger for the burst of THz technology in the 1990s was the optical-to-THz conversion technology using lasers [10,11]. Although laser pumped THz sources usually have limited conversion efficiency because of the huge quantum defect from laser to THz frequency, significant progress has been made in the past two decades with the development of laser technology and conversion media. This review discusses the basics and development of optically pumped THz sources. It should be noted that as all the optical pump sources for THz generation are lasers, "optically pumped" is identical to "laser pumped". Moreover, gas THz lasers pumped by IR lasers are also optically pumped, so they are included as well and novel ideas to improve these antiquated facilities are introduced in this paper.

2 Ultrafast THz sources

Ultrashort THz sources derived from femtosecond lasers producing coherent few-cycle THz pulses, are an important class of THz sources enabling time-domain spectroscopy (TDS). THz TDS has the unique ability to characterize the complete electric field of a THz pulse with full phase and amplitude information, thus the complex dielectric function of a sample can be determined directly without having to rely on Kramers-Kronig (K-K) relations, a great advantage over Fourier transform infrared spectroscopy (FTIR) that gives only the intensity measurement. With these advantages, THz TDS not only helps identifying chemical or biochemical molecules, but also provides a powerful tool for imaging in pharmaceutical, security, or scientific identification of substances such as drugs, explosives or weapons. THz imaging with TDS is implemented into quality control and optimization of industrial manufacturing processes (http://www.menlosystems.com/). High-field-strength ultrashort THz pulses also enable new approaches of studying the physical processes of condensed matters [7].

The most widely used techniques of generating ultrafast THz pulses are photoconductive switch (antenna) [12] and optical rectification [13], which can be pumped with either femtosecond oscillators or amplified systems for single- of few-cycle THz pulses. There is also a promising method to obtain very short single-cycle THz pulses with high-field strengths by nonlinear processes in gas plasmas [14]. Despite of some other THz generating methods like semiconductor surface emitters [15], in this part we will concentrate the discussion only on three main ultrafast THz pulse generating techniques.

2.1 THz generation by photoconductive switch

As the most widely used method for the generation and detection of THz pulses in TDS, the photoconductive switch was firstly introduced by Auston and Smith in the early 1980s [16]. A photoconductive switch consists of two short metallic stripes with a small gap (around 10 μm) in between, placed on a semiconductor substrate with a short charge carrier lifetime, as shown in Figure 1. A direct current (DC) bias voltage (10–50 V) is applied to the stripes. A visible or near-IR femtosecond laser is focused in this region between the metallic stripes creating a closed circuit for a short time. The fast change in polarization P induces fast oscillations with a field strength of $E_{\mathrm{THz}} \propto \mathrm{d}^2P/\mathrm{d}t^2$, which in turn leads to THz emission in a wide range of angles through the switch composed by the resistance-capacitance (RC) circuit with response time on the order of a picosecond. Photoconductive switches have been continuously improved since the early works, greatly increasing the THz pulse energy and frequency response by using novel switch material, geometry and optimizing the photoconductive area.

The emitted THz pulse is proportional to the second derivative of the transient current inside the switch, the pulse duration of the femtosecond laser and the carrier rise time intrinsic to the material. The preferable material for the most commonly used Ti:Sapphire femtosecond laser at 800 nm is gallium arsenide (GaAs), which has a fast carrier rise time, high mobility and a smaller band gap (1.42 eV) than the laser photon energy (1.55 eV). As a great improvement, low-temperature (LT) grown GaAs by molecular beam epitaxy (MBE) has been widely used to overcome the slow photo-response time of conventional semiconductors [17]. The LT-GaAs has a carrier lifetime shorter than 500 fs (even reaching the sub-100-fs duration) and high resistivity [18], yielding a

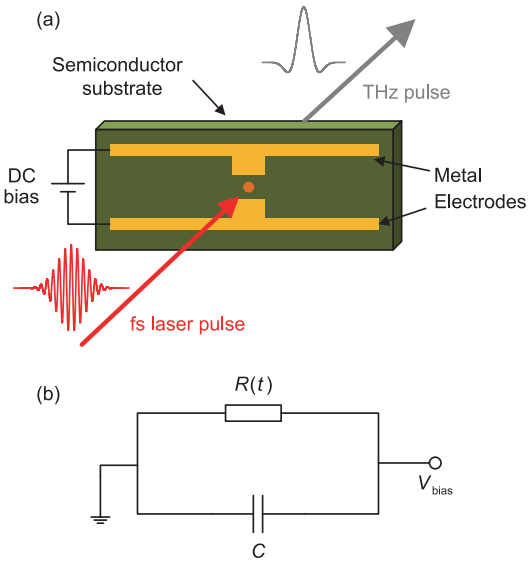

Figure 1 (Color online) Schematic diagram of THz pulse emission from a photoconductive switch excited by a femtosecond laser pulse. (a) Schematic diagram; (b) equivalent RC circuit.

spectrum typically in the range of 0.1–3 THz, limited mostly by the laser pulse duration, material absorption and dispersion. A number of semiconductor materials besides GaAs, like Si, InAs, InP, ZnSe and ZnTe, have also been used in photoconductive switches. For THz generation with 1.5 μm fiber lasers, InGaAs/InAlAs multi-layer structures have been developed [19], and the bandwidth can be improved up to 4.5 THz with a peak dynamic range larger than 70 dB [20].

Various antenna geometries besides the Auston switch have been discussed, including the bow-tie antenna, interdigitated structures, spiral antenna and other more sophisticated designs derived from microwave theory. With stronger femtosecond amplifiers, THz energy scaling is feasible by enlarging the switch gap to the order of 1 cm and increasing the bias voltage to several kV. As a result, strong THz pulse energies of 800 and 400 nJ were achieved at 10 Hz and 1 kHz repetition rates with GaAs photoconductive switches [21,22]. However, large aperture antennas are limited by various technical factors including thermal instability, lack of reliability and saturation at low pumping fluence, etc. Recent research focused on enhancing THz generation by implementing an interdigitated geometry and incorporating nanoantennas or plasmonic electrodes, enabling much higher optical-to-THz conversion efficiencies of up to 7.5% with a maximum output power over a milliwatt [23–25]. Wide-bandgap semiconductor crystals allowing larger bias fields are also exploited to improve the radiated THz pulse energy. Using a ZnSe large aperture photoconductive antenna (12.2 cm^2) illuminated by a 400-nm pump laser at 10 Hz, THz pulses with energy of 8.3 μJ were obtained corresponding to electric field up to 331 kV/cm [26].

2.2 THz generation by optical rectification

Optical rectification (OR) is a second-order nonlinear optical process first demonstrated in 1962 [27], soon after the invention of lasers. It is based on the inverse second-order electro-optical effect in a nonlinear crystal and can be considered as difference frequency generation (DFG) between the spectral components of a broad bandwidth femtosecond laser, instead of two monochromatic pumping beams. Since the first discussion on far-IR generation using OR based on picosecond laser pulses and a $LiNbO_3$ crystal in 1971 [28], this THz generating technique has been steadily developed and greatly improved by the leaps of femtosecond lasers.

In the OR process, the nonlinear polarization induced by the pump laser pulse is expressed as [29]

$$P_{\mathrm{NL}}(\Omega) = \varepsilon_0 \chi^{(2)} \int_0^{\infty} E(\omega+\Omega)E^*(\omega)\mathrm{d}\omega, \tag{1}$$

where ε_0 is the free space permittivity, $\chi^{(2)}$ is the second-order nonlinear susceptibility of the medium, $E(\omega)$ is the Fourier-component of the pump pulse (ω>0), ω and Ω are the frequencies of the laser and THz pulses. Phase-matching (PM) conditions should be satisfied for efficient OR, described as [30]

$$\Delta k = k_{\Omega} + k_{\omega} - k_{\omega+\Omega}, \tag{2}$$

where k is the wave vector for each wavelength. Since $\Omega \ll \omega$, $k_{\omega+\Omega} - k_{\omega} \approx \partial k / \partial \omega\big|_{\omega_0} \cdot \Omega$, which gives $\Delta k = \left[n(\Omega) - n_{\mathrm{g}}(\omega_0)\right]\Omega / c$ in the case of collinear THz generation. Here ω_0 is the mean pump frequency, c is the speed of light in vacuum, n and n_{g} are the refractive index and group index, respectively. According to the second-order nonlinear optical principles, the efficiency of OR is highly dependent on the figure of merit (FOM) of the nonlinear material [7]. A vast group of non-centrosymmetric crystals with high FOMs have been investigated for OR [7], including $LiNbO_3$, $LiTaO_3$, GaSe, organic crystals DAST, BNA and OH1, and zinc blende crystals ZnTe, GaP, GaAs, ZnSe, CdTe, etc.

Organic crystals have large nonlinear coefficients, but the THz absorption is also very strong and the damage threshold is limited. The most commonly used material for OR is ZnTe [31], owning the merits of a high FOM value and collinear PM for Ti:Sapphire laser pumping. It is a similar case for GaP pumped by Yb doped 1-μm lasers [32], and GaAs pumped by Er-doped 1.56-μm fiber lasers [33]. For fiber lasers with a longer wavelength of 2 μm, orientation-patterned GaAs can be used as an efficient THz conversion material [34]. Stoichiometric $LiNbO_3$ crystals are another category of popular nonlinear materials for OR, taking the advantages of high FOM values and large bandgap allowing only three-photon absorption for 800 nm pumping. However, the THz refractive index for $LiNbO_3$ is significantly larger than the optical

group index, and therefore collinear PM is impossible. In order to enhance efficiency, quasi-phase-matching (QPM) in periodically poled $LiNbO_3$ (PPLN) was used to enhance efficiency, resulting in multi-cycle THz pulses [29].

Tilted-pulse-front pumping geometry, which should be recognized as the best scheme for powerful THz generation in bulk $LiNbO_3$, was firstly proposed in 2002 [35]. In the geometry of tilted pulse front shown in Figure 2(a), the generated THz wave propagates perpendicularly to the pulse front with THz phase velocity $v(\Omega)$, leading to noncollinear PM condition if $v_g\cos\gamma=v(\gamma)$ is satisfied. Apparently, PM can be achieved by choosing a particular tilt angle γ in the case of $LiNbO_3$ where $n_g(\omega_0)\leq n(\Omega)$. On the other hand, the THz frequency can be tuned by changing this angle. Compared with OR using ZnTe, power scaling of $LiNbO_3$ with tilted-pulse-front does not exhibit saturation until very high pump energies are reached. For example, pumping at 800 and 1030 nm, high energy THz pulses approaching millijoule level were realized lately and the conversion efficiency was over 1% [36–38]. Such powerful THz pulses are of great use in many aspects and make it possible to research THz nonlinear effects.

Another PM method for OR is the Cherenkov geometry. Cherenkov radiation was predicted by Askar'Yan [39]. A Cherenkov-like cone can be generated by an electromagnetic pulse in dispersive medium via nonlinear effects. This geometry of radiation accompanying nonlinear optical effects can also be considered as a kind of PM. When the pump laser is focused into a nonlinear crystal like $LiNbO_3$ or $LiTaO_3$, THz radiation moving with the pulse envelop is produced by OR [40,41]. As the refractive index of THz waves is larger than that of the pump laser, the velocity of the pump exceeds that of the THz radiation, so that Cherenkov condition is satisfied. As shown in Figure 2(b), the THz wave from bulk $LiNbO_3$ or $LiTaO_3$ is generated with a tight focusing point or line, and the same PM condition is obtained for pulse-front-tilt angles θ_c. However, collimating the conic generated THz wave is difficult for this, and Cherenkov PM does not allow the use of extended pump spot [41]. Wedged radiation by line pump source instead of conic radiation was also investigated using cylindrical lens to focus the pump pulse, and the efficiency was increased to 10^{-4} [42,43]. A further improvement is to use a planar waveguide structure, which consists of a thin high nonlinear core cladded with a low-absorption lens, enabling the increase of the effective radiation length and outcoupled THz power. With this method, the conversion efficiency was increased up to 10^{-3} and the frequency range covered was 0.1–7 THz [44,45]. P-polarized Cherenkov radiation with Brewster-cut geometry was also discussed, which can provide high coupling efficiency, high intensity and good beam quality [46]. Overall, tilted-pulse-front PM usually gives much higher energy of THz pulses and is advantageous over Cherenkov PM.

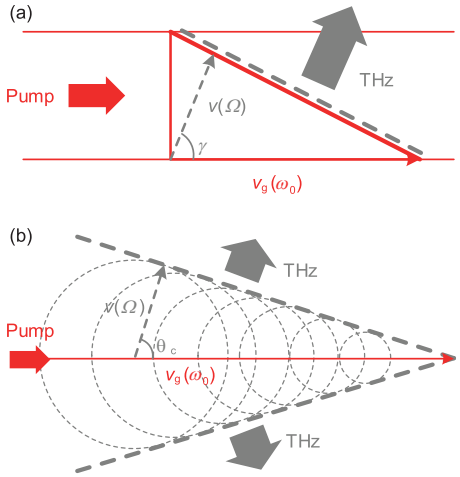

Figure 2 (Color online) OR PM via (a) tilted pulse front and (b) Cherenkov geometry. The solid and dashed lines denote pump and THz waves, respectively. The thick lines indicate phase front and the arrows indicate the propagation direction and velocities.

2.3 Gas-based wide-band THz generation

Laser-induced gas plasma can be used to generate intense, coherent, broadband, and highly directional THz waves through a nonlinear optical process [7,47,48]. THz generation in plasma has the advantages that there is no damage threshold for gas and the available bandwidth is only limited by the duration of the pump laser since no material absorption needs to be considered. Furthermore, the THz pulses can also be detected in gases using THz induced second-harmonic generation (SHG) of fluorescence.

When a laser pulse is focused into a gas with intensity above a critical value near 10^{14} W/cm^2, the ionized gas contains positively and negatively charged particles (plasma), which emits a broad continuum of coherent and incoherent radiation. Although pulsed CO_2 lasers capable of ionizing air were introduced in the 1970s, the optical pulse durations were insufficiently short for THz wave generation. The first report on far-IR or THz generation using laser plasmas was in 1993 by Hamster et al. [49], with TW level femtosecond lasers. In 2000, there was a significant progress in efficiency using this approach of mixing of femtosecond pulses with their SHG wave inside the plasma, giving THz fields estimated to be 2 kV/cm [50]. In 2008, Kim et al. [51] reported the coherent control scheme to optimize THz generation in gases and the obtained THz pulse energy was up to 5 μJ with a conversion efficiency of over 10^{-4}. With shorter pump pulse duration of 19 and 10 fs, the THz bandwidth was extended to 100 and 200 THz, far beyond the THz range [52,53]. The energy conversion efficiency reached 7×10^{-4} by expanding the plasma source into a two-dimensional sheet [54].

A common gas-based THz generation experimental scheme is shown in Figure 3. An 800-nm mode-locked Ti:Sapphire laser amplifier with a pulse energy of mJ-level is focused by

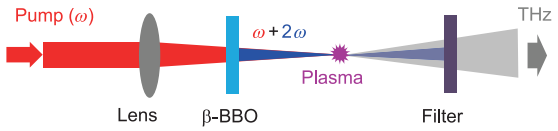

Figure 3 (Color online) Experimental scheme of THz generation in gas plasma driven by two-color lasers.

a spherical lens into a gas target to excite plasma. Before the focus, a beta-barium borate (β-BBO) crystal was used for SHG at 400 nm. According to the four-wave-mixing (FWM) description [50], the mixed fundamental and second harmonic beams (ω and 2ω in frequency, respectively) generate an ionizing plasma spot that emits intense, directional, ultra-broadband THz radiation. The THz field satisfies $E_{\mathrm{THz}} \propto \chi^{(3)} I_{\omega} \sqrt{I_{2\omega}}$ under relatively low laser peak power intensities. Pure nitrogen or noble gases (Kr or Xe) with higher tunnel ionization rates can significantly improve the efficiency by getting rid of the water vapor in air [51].

When the laser intensity is very high, however, the above FWM approximation is no longer valid [55]. Although FWM is a convenient framework for experimental results because of simplicity, more sophisticated models are required to explain the observed THz field strength as well as the existence of intensity threshold. Kim et al. [56] and Roskos et al. [57] treated it semiclassically, assigning the generation process to the formation of a current or polarization of the ionizing electrons, respectively. A two-step model was also proposed to deeply reveal the rather complex phenomenon of THz generation in plasma by a two-color laser field [58]. There were also explanations that put forward recently on how the plasma current oscillation and photocurrents driven by two-color lasers impacted broadband THz generation [59–62]. Continuous research for a complete description is still going on for this topic.

3 Monochromatic THz generation by DFG

DFG is another method to generate THz waves in second-order ($\chi^{(2)}$) nonlinear materials other than OR. DFG is a process that converts two optical frequencies ω_1 and ω_2 ($\omega_1 \approx \omega_2 = \omega_0$) into a THz frequency ω_{THz} (here ω_{THz} is used for monochromatic THz wave instead of Ω which is used in 2.2 for broadband THz wave). The pump lasers for DFG are usually nanosecond, picosecond or even continuous-wave (CW) monochromatic lasers, in contrast to the broadband femtosecond lasers used in OR, thus the group velocity dispersion for DFG is insignificant. Benefiting from the spectral purity and tunability, DFG sources are extremely useful to resolve the narrow-linewidth rotational transitions of low-pressure gases and fingerprint the molecules exhibiting congested and unresolved rovibrational spectra. It is also feasible to take multispectral images of targets and analyze the targets based on the THz spectra with DFG sources [8].

Considering the plane-wave model in the small-signal approximation and neglecting all the reflections and absorptions, the THz intensity generated in DFG process is

$$I_{\mathrm{THz}} = \frac{2\omega_{\mathrm{THz}}^2 d_{\mathrm{eff}}^2 l^2}{\varepsilon_0 c^3 n_{\mathrm{opt}}^2 n_{\mathrm{THz}}} I_{\mathrm{opt}}^2 \cdot \mathrm{sinc}^2\left(\frac{\Delta k l}{2}\right), \tag{3}$$

where I_{opt} and I_{THz} are the incident laser intensity and generated THz intensity inside the nonlinear crystal, d_{eff} is the efficient nonlinear coefficient, l is the interaction length, n_{opt} and n_{THz} are the refractive indices at optical and THz frequencies. There are quite a few factors limiting the overall conversion efficiency. First, the large quantum defect (on the order of 100) from laser to THz; Second, a high THz absorption coefficient (a few to tens of cm^{-1}) in most nonlinear materials; Third, the wave vector mismatch of the three-wave interaction process due to dispersion: $\Delta k = k_1 - k_2 - k_{\mathrm{THz}}$, similar to eq. (2). While the other limitations are inherent and have no practical solutions, PM (Δk=0) should be the first thing to be considered in DFG.

Taking collinear DFG ($\omega_1 - \omega_2 = \omega_{\mathrm{THz}}$) in a crystal that exhibits normal dispersion as an example, the PM condition is

$$\Delta k = \frac{n_1\omega_1}{c} - \frac{n_2\omega_2}{c} - \frac{n_{\mathrm{THz}}\omega_{\mathrm{THz}}}{c}. \tag{4}$$

Incorporating with the energy conservation condition we can rewrite this equation into

$$\Delta k = \frac{1}{c}[\omega_1(n_1 - n_2) + \omega_{\mathrm{THz}}(n_2 - n_{\mathrm{THz}})]. \tag{5}$$

According to normal dispersion $n_1 > n_2$ and $n_2 > n_{\mathrm{THz}}$, the overall expression is always a positive quantity so that strictly $\Delta k > 0$ and this process will not be phase matched. However, the current discussion is limited to isotropic media or birefringent medium where all the fields are e-waves or all the fields are o-waves. On the other hand, using differently polarized beams in birefringent materials, in non-collinear configuration or if normal dispersion is not valid which is often the case in THz generation, PM becomes possible. On account of different materials suitable for DFG from IR into THz wave, various PM methods have been developed, which will be discussed in the following text.

3.1 Birefringent PM

In birefringent materials, since the different k-vectors can be either o- or e-polarized, PM can sometimes be achieved by choosing different propagation directions in collinear interactions. The first successful far-IR DFG in the 1960s with quartz and $LiNbO_3$ as the nonlinear materials used birefringent PM [63,64]. However, quartz and $LiNbO_3$ have serious absorption in the THz range, low effective nonlinear coefficients and limited PM range, thus the output power and tunability were quite limited. With the development of IR nonlinear materials, high-quality large-size GaSe and ZGP

crystals with large efficient nonlinear coefficients have been adopted in THz generation, greatly improving the DFG efficiency.

GaSe has low THz absorption, large nonlinearity and large birefringence, enabling widely tunable high power THz output. In 2002, Shi et al. [65] reported 0.18–5.27-THz tunable THz generation by DFG in a 15-mm-long GaSe crystal, using a Nd:YAG pulsed laser and a tunable β-BBO based master oscillator-power oscillator (MOPO) around 1.06 μm as the pump source. They improved the output power to 389 W and a broader tunable range in the low-frequency end to 0.053 THz with longer crystals [66]. Under different PM schemes, widely tunable mid-IR pulse was generated extending the output wavelength to 2.7 μm [67]. Tunable backward-propagating THz generation was also observed benefitting from the large birefringence of GaSe crystals [68].

To increase the sampling rate in THz applications, high-repetition-rate operation is needed. With bulky and complicated high-power CO_2 laser systems working at 60 kHz near 10 μm, high THz output average power of 260 μW at 328.2 μm was successfully realized in 2008 [69]. Single-frequency Q-switched fiber lasers around 1550 nm were also used to generate μW-level THz waves at 200 μm [70]. Zhao et al. [71,72] discussed THz generation from a compact solid-state laser system using Nd:YLF crystals which gave simultaneous dual-wavelength output at 1047 and 1053 nm. However, Nd:YLF lasers were incapable of wavelength tuning and the timing jitter is usually ineluctable. The timing jitter problem can be solved by a coaxial pumping configuration [73], which is much more stable, flexible and compact. Recently, we investigated THz generation from tunable 2-μm degenerate OPOs intracavity pumped by 1064-nm lasers. Following the first attempts with electro-optical Q-switched Nd:YAG lasers [74], compact acousto-optical Q-switched Nd:YVO_4 lasers were then used to pump OPOs for high-repetition-rate operation, as shown in Figure 4. Degenerate 2-μm lasers are simple, efficient, widely-tunable and their short pulse duration is good for enhancing DFG efficiency. They are one of the best candidates for DFG while compact powerful mid-IR dual-wavelength lasers are not available. A tunable range of 0.41–3.71 THz was achieved with a walk-off compensated KTP OPO [75], and when the KTP crystals were replaced with a 14.1-μm-grating-period type-II QPM PPLN crystal, the tunable range was even wider (0.24–3.78 THz), owing to a better beam quality and a more precise wavelength tuning method [76]. The maximum output powers were in the microwatt range, good enough for spectroscopy and imaging applications.

$ZnGeP_2$ (ZGP) is another commonly used birefringent material in DFG for THz waves generation. ZGP has good physical properties and can be cut at required PM angles which are impossible for GaSe. However, the absorption coefficients of ZGP at 1 μm and in the THz range are much higher than those of GaSe and high-quality large-size crystals are rather difficult to grow, which constrain its frequency tunability and power scaling. Hundred-Watt-level THz peak power was reported by Shi and Ding [77] in ZGP based on pulsed lasers. BAE Systems also reported high average power of 2 mW based on two all-fiber laser amplifier chains [78], which was among the highest power records for DFG THz sources.

3.2 Noncollinear PM

Some isotropic bulk nonlinear semiconductors such as GaAs, InSb, GaP, ZnSe and ZnTe have large nonlinearities and have good potential for THz DFG. These crystals lack birefringence, so 'PM' is only satisfied within one coherence length, the distance over which the relative phase changes by π. For THz generation, the coherence length is quite long, for example, it is on the order of 1 mm in the case of GaAs, thus it allows the generation of THz in thin slabs, but clearly the power is very limited [79,80]. In some cases PM can be satisfied because of the presence of reststrahlen band, but such applications are limited to certain wavelength and are not convenient to use. Another approach to obtain PM THz DFG in isotropic nonlinear materials is the noncollinear mixing of two laser beams. For the wave vector triangle shown in Figure 5, the PM conditions are given by [81]

$$\sin\frac{\theta}{2}=\left[\frac{n_3\omega_{\mathrm{THz}}^2-(n_1\omega_1-n_2\omega_2)^2}{4n_1n_2\omega_1\omega_2}\right]^{1/2}, \tag{6}$$

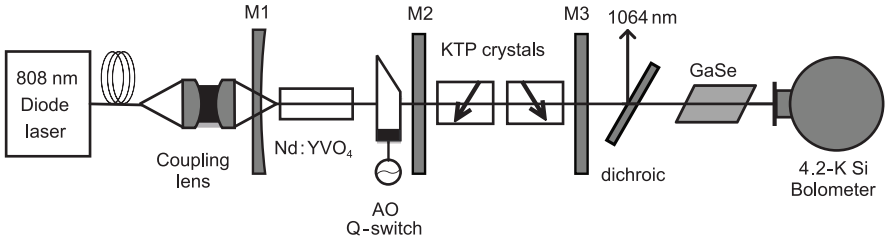

Figure 4 Experimental setup for the high-repetition-rate THz DFG system based on a intrcavity pumped dual-wavelength 2-μm KTP OPO and a GaSe crystal.

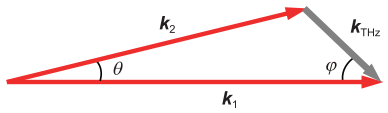

Figure 5 (Color online) Wave vector PM triangle of the noncollinear DFG.

$$\cos\varphi = \left[1+2\frac{\omega_2}{\omega_{\mathrm{THz}}}\sin^2\left(\frac{\theta}{2}\right)\right] \times\left[1+4\frac{\omega_1\omega_2}{\omega_{\mathrm{THz}}^2}\sin^2\left(\frac{\theta}{2}\right)\right]^{-1/2}, \quad (7)$$

from which the PM angles can be calculated for experimental layout.

Most of the noncollinear DFG schemes for THz generation are based on CO_2 laser systems around 10 μm. Longer pump wavelengths are good for enhancing conversion efficiency by an order. The pioneering work for noncollinear DFG were demonstrated in the 1970s [79,82], where GaAs was used for THz generation, giving a few kilowatts in peak power at most in the 3 THz region with a cryogenically cooled sample. In 2005, the record-level 2 MW peak power was achieved in UCLA with significantly improved damage threshold using 250-ps pump pulses [83], corresponding to a conversion efficiency of 10^{-3}. In 2007 they also reported efficient 0.5–3-THz tunable THz generation using typical 200 ns pulses [84], giving maximum THz pulse energy of 400 μJ in the spectral range of 0.5–2 THz, corresponding to a peak power of 2 kW. Generally speaking, noncollinear PM DFG in semiconductors based on powerful CO_2 lasers has obvious advantages in THz pulse energy and peak power. However, as these systems are usually extremely bulky and the repetition rate is very low compared with solid-state or fiber lasers, so that their applications are not convenient.

There is the other kind of noncollinear DFG scheme where the dispersion of phonon-polariton mode modes are involved in relation to PM. With this method, frequency-tunable THz sources were obtained from GaP crystals using an optical parametric oscillator and a Nd:YAG laser at 1.064 μm as the dual-wavelength pump source [85–87]. By tuning the angle between the two pump beam directions, tunable THz wave covering the frequency range from 0.5 to 7 THz were achieved with the peak power up to hundreds of milliwatts.

3.3 QPM

QPM provides a much more flexible technique to achieve PM that does not require birefringence, which was proposed even before birefringent PM [88]. QPM crystals periodically reset the phase of the nonlinear polarization, commonly via changing the crystal's nonlinearity $\chi^{(2)}$ to maintain a coherent build-up of the nonlinear interaction. The PM condition becomes

$$\Delta k = k_1 - k_2 - k_{\mathrm{THz}} - k_\Lambda = 0, \quad (8)$$

$$k_\Lambda = 2\pi m/\Lambda, \quad (9)$$

where k_{m} is the wave vector introduced by the modulated nonlinearity, Λ is the QPM period, and m is the QPM order which is only meaningful if it is an odd number. The k_Λ term gives another degree of freedom to compensate phase mismatch and can be designed into whatever is required. Therefore, QPM enables flexible PM throughout the whole transparent range of the material which is a great advantage compared with birefringent PM, and the largest nonlinear coefficient can be utilized by choosing the optimal propagation direction and polarization of the interacting waves, favorable in power and conversion efficiency scaling. It should be mentioned that not only cubic crystals, but birefringent ferroelectric crystals are also suitable in QPM without walk-off. Practical methods to achieve QPM by rephrasing the nonlinear polarization include stacking crystal plates with periodical rotations of 180° [89], periodical poling (PP) [90], orientation-patterned (OP) epitaxial growth [91], etc.

As the most commonly used QPM crystals, PPLNs have been used for generating tunable THz waves, either in the forward or backward DFG [92]. The main problem is that THz absorption in $LiNbO_3$ material is extremely high, and to overcome this disadvantage, surface-emitting geometries with slant-stripe PPLN design can be used [93], as shown in Figure 6. Using a dual-wavelength vertical external cavity surface emitting laser (VECEL) as the pump source, milliwatt level high-power CW THz sources were realized through DFG with a surface-emitted PPLN crystal inside the laser cavity [94].

Zinc blende semiconductors like GaAs and GaP crystals are of much more interest because of their higher nonlinear coefficient and much lower THz absorption. They are grown or manufactured into QPM device using orientation-patterned epitaxial growth, diffusion-bonding or optical contacting techniques [95]. Periodically inverted GaP, which has a wide transparent range at short wavelength in the near-IR, was investigated for THz generation pumped with 1-μm or 1.5-μm lasers with photon conversion efficiency reaching up to 40% [96–98]. GaAs, however, has a strong two-photon absorption below 1.75 μm but lower absorption in the THz range and a much higher nonlinear coefficient. With almost the same experimental setup as in Figure 4 and a 1.3-mm-period QPM GaAs sample, we obtained micro-watt level THz generation at around 1.244 THz. Intracavity pumped by high-power picosecond [99] and CW dual-wavelength 2-μm lasers [100], efficient optical-to-THz DFG was realized in QPM-GaAs samples with the maximum average output power reaching 1 mW.

3.4 Cherenkov PM

Similar to Cherenkov PM OR introduced in Section 2.2, Cherenkov PM can also be utilized in monochromatic THz

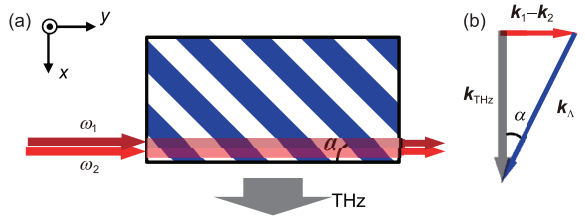

Figure 6 (Color online) Schematic of a slant-stripe PPLN used for surface-emitted THz generation (a) and the wave vector PM relation (b).

generation via DFG with dual-wavelength pulses and $LiNbO_3$ crystals, and here it is more like a kind of PM geometry rather than Cherenkov radiation. The only difference in the scheme is two monochromatic laser pulses are used as the pump instead of only one ultrafast wide-band laser pulse. The detailed theoretical analysis for Cherenkov PM DFG with nanosecond laser pulses is given in ref. [101]. The Cherenkov angle θ_c is determined by $\cos\theta_c=n_{opt}/n_{THz}$.

The first demonstration of Cherenkov DFG was in 2008 [102]. A dual-wavelength OPO pumped by a frequency doubled Nd:YAG laser was used as the pump source and it was focused into a 5 mol% MgO:$LiNbO_3$ crystal. A Si prism was used to couple the generated THz radiation, giving a tuning range of 0.2–3 THz with the highest THz pulse energy of 80 pJ. It was also concluded that tight focusing is required to avoid destructive interference caused by extended THz generation with a large pump beam [103]. However, tight focusing also causes severe divergence and pump diffraction. Several methods to improve the tuning range and conversion efficiency have been proposed. One method was to use waveguide structure, within which a wide tuning range of 0.1–7.2 THz was achieved [104]. Another was the surface emitting configuration by total internal reflection, which enabled 0.2–6.5 THz tuning range and a conversion efficiency of 7-folded by greatly reducing THz absorption at the surface [105]. With an improved dual-wavelength KTP OPO, the maximum THz output energy was improved to 1.58 nJ at 0.78 THz using Cherenkov PM DFG recently [106].

3.5 DFG with organic crystals

As mentioned in Section 2.2, organic crystals usually exhibit very good nonlinear optical properties such as larger nonlinearity and wider frequency response than those of inorganic nonlinear crystals. A few kinds of organic crystals such as DAST [107], DASC [108], DASB [109] and BNA [110], have been developed and exploited in widely tunable THz generation covering 0.1–30 THz. It is also important to achieve PM DFG for better efficiency in organic crystals, but there are several limitations for practical applications, e.g. large crystals are hard to grow and manufacturing is almost impossible because limited by the physical properties of organic crystals. Therefore, DFG is usually conducted within one coherence length along the so-grown *c*-axis. Another point to mention is to use the largest nonlinear coefficient d_{11}, two pump beams should be parallel polarized to the crystallographic *a*-axis [107]. Taking DAST for example, collinear phase-matching can be achieved with input wavelengths centered at 1.15 μm to generate THz frequencies. The coherence length for the 0.5–1 THz generation was longer than 1 mm pumped at the 1.02–1.50 μm wavelength range [111], which is good enough for DFG considering its large nonlinearity and high absorption.

In 2007 Ito et al. [112] reported ultra-broadband (1.5–37 THz) THz wave generation using DFG in an DAST crystal based on a dual-wavelength optical parametric oscillator (OPO) with two KTP crystals pumped by a frequency doubled Nd:YAG laser, giving 10 nJ pulse energy at around 26 THz. Liu and Merkt [113] realized Fourier-transform-limited (10 MHz bandwidth) THz pulses in DAST crystals with peak power up to 400 μW pumped by two narrow-band Ti:Sapphire lasers and a b-cut DAST crystal to fulfill the PM condition, which was used to distinguish water absorption lines and a pure rotational transition of HF. As a much simpler scheme, simultaneous dual-wavelength Nd:YAG laser operating at 1319 and 1338 nm can be used to generate 3.2 THz pulses, and recently we realized a ultra-compact THz source with this scheme for portable applications [114].

In the past few years, THz generation in the derivatives of DAST have been investigated in some Chinese universities and institutes, e.g. DSTMS and OH1, which have even better properties on crystal quality and THz absorption than DAST. Pumped by dual-wavelength KTP OPOs in the wavelength around 1.3 μm, the obtained maximum THz pulse energy was up to 85.3 and 507 nJ respectively, and the frequency range covered 0.02–20 THz in the latest results [115,116].

3.6 DFG in waveguides

Isotropic crystals can also be manufactured into waveguide structures for PM. A pioneering work was reported by Thompson and Coleman [117], giving THz output from a planar GaAs waveguide with a nanowatt range average power (1-mW in peak) by mixing CO_2 laser lines. Since then, various planar, ribbed and slotted GaAs/GaP waveguides have been investigated theoretically and experimentally for widely tunable and high-power THz generation from DFG satisfying the PM condition [118–123]. Benefiting from the flexible designs of waveguides, the whole THz wave frequency range can be covered with relatively high average power and diversified polarizations. Cherchi et al. [124] performed a detailed material comparison on dielectric waveguides made of zinc-blende semiconductors for guided-wave THz DFG. Saito et al. [125] studied PM DFG based on a silicon waveguide with strain induced second-order nonlinearity, demonstrating promising applications for high-power THz sources. Another silicon-based waveguide proposed by Baehr-Jones et al. [126] used high-nonlinearity

polymer cladding to mix the IR lasers, giving the possibility of CW THz generation. Sinha et al. [127] reported a widely tunable room temperature THz source based on nonlinear mixing in a hybrid optical and THz micro-ring resonator in order to enhance THz generation compared with bulk nonlinear material by using the high second order optical susceptibility ($\chi^{(2)}$) in crystals and polymers, which is prospective for on-chip integrated systems.

In addition to PM, waveguides also provide good approaches for improving the DFG efficiency and output THz intensity with much better mode confinement compared with bulk materials. Ding theoretically analyzed metallic-dielectric hybrid (MDH) waveguide to significantly enhance the strengths of the interactions for several THz parametric processes by eliminating the diffraction of the THz waves as well as reducing the modal indices, either in forward or backward generation [128]. Liu et al. [129] investigated a nonlinear crystal fiber converter for THz DFG consisting of a periodically inverted GaAs core clad with index-matched chalcogenide glass, which worked as a single-mode fiber high-brightness THz source with efficient optical-to-THz conversion.

3.7 Cavity-enhanced DFG

In THz generation based on single-pass configurations through nonlinear crystals, the conversion efficiencies are typically very low because the pump intensity is quite limited, while the generated THz intensity has a quadratic relation to the pump intensity. However, as the power of pump lasers is usually limited, it is very important to efficiently and coherently recycle the laser pulses to obtain high-power THz generation. This can be realized by an external enhancement cavity as shown in Figure 7. The enhancement cavity can be optimized to provide small cavity round trip losses (Δ) in order to maximize the enhancement factor. The maximum enhancement factor A for the pump intensity under the condition of mode matching in the CW case is given by [130]

$$A = \frac{1-R}{\left[1-\sqrt{R(1-\Delta)}\right]^2 + 4\sqrt{R(1-\Delta)}\sin^2\left(\frac{\delta}{2}\right)}, \tag{10}$$

where R is the reflectivity of the cavity and δ is the phase difference between two consecutive round trips. The highest enhancement factor is reached for impedance matching (R=1−Δ) and constructive interference (δ=0), which means the cavity length should be stabilized within a difference of a fraction of 1 μm.

Femtosecond, nanosecond and CW steady state lasers have been studied in external cavity-enhanced nonlinear frequency conversions [131–133], all of which reached high enhancement factors. In 2010, NP Photonics Inc. reported a resonant external cavity approach to enhance narrowband THz radiation through DFG from two nanosecond 1.5-μm lasers that

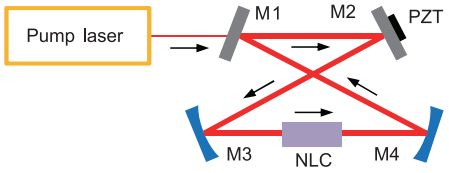

Figure 7 (Color online) Bow-tie external enhancement cavity for nonlinear optical frequency conversion. M1–M4: cavity mirrors. M1 has partial transmission and the others are high-reflection coated for the pump. PZT: piezo for fine tuning the cavity length. NLC: nonlinear crystal.

were resonant in an optical cavity and interacting with a ZGP crystal [134]. An enhancement factor of 7 was produced for the THz power compared with a single-pass orientation. In 2011, they made significant progress using QPM GaP, from which an enhancement factor of approximately 250 was achieved compared with single-pass THz DFG [98]. The maximum THz average power reached 339 W, corresponding to a power conversion efficiency of 2.43×10^{-4} and a quantum efficiency of 3.16%. External cavity enhanced DFG demonstrates great advantage in the case of low-power pumping, which enables CW THz generation through DFG for a much higher optical-to-THz conversion efficiency [135].

3.8 Cascaded DFG

Although various methods have been developed to increase the DFG conversion efficiency from near IR to THz, the inherent large quantum defect is always a great barrier preventing further improvement. Cascaded DFG is a promising approach because more than one THz photons can be produced for one pump photon depletion, making it feasible to break the Manley-Rowe limit. The basic concept is shown in Figure 8. If the initial pump intensity and generated THz intensity are high enough, the DFG process will continue to generate new frequencies, making further DFG process possible and enhancing the total THz intensity by constructive interference. Efficient cascading gives a possible approach to improve the DFG efficiency inherently.

The application of cascaded DFG to the enhancement of THz generation was firstly predicted by Cronin-Golomb where ZnTe and 800 nm laser were used in the discussion [136]. Later, this cascading phenomenon was observed with QPM GaAs in a intracavity DFG configuration [137], however, the actual enhancement was unconspicuous. We analyzed the detailed dynamic process in both isotropic crystals and QPM crystals [138,139], giving the optimal designing parameters for cascaded DFG. Cascaded Cherenkov-type DFG in a sandwich-like waveguide was also proposed to overcome the phase mismatch and provide efficient output coupling [140]. Recently, Ravi et al. [141] gave feasible designs on a highly efficient (over 10% conversion efficiency), practical approach to high-energy multicycle THz generation

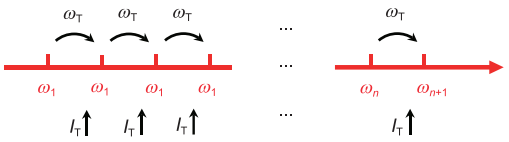

Figure 8 (Color online) Schematic of the cascaded DFG process starting from two initial pump frequencies ω_1 and ω_2.

in cryogenically cooled PPLN based on spectrally cascaded optical parametric amplification (THz-COPA), initially generated by DFG between a narrowband optical pump and optical seed (0.1%–10% of pump energy). This approach paves the way for extremely high-energy THz sources.

4 THz generation from stimulated polariton scattering

When laser beams propagate through nonlinear crystals, the photon and phonon transverse wave fields are coupled and behave as new mixed photon-phonon states—polaritons. THz radiation can be generated from the efficient parametric scattering of laser light via polaritons. This effect is the so-called stimulated polariton scattering (SPS), which occurs when the pump excitation is sufficiently strong in polar crystals like $LiNbO_3$ and GaP with transverse optical phonon modes that are both IR- and Raman-active. The scattering process involves both second- and third-order nonlinear processes. Consequently, strong interaction occurs between the pump beam, the idler beam and the polariton (THz) waves, enabling a method of efficient THz parametric generation.

As shown in Figure 9 [142], polaritons exhibit phonon-like behavior in the resonant frequency region (near the TO-phonon frequency ω_{TO}). However, they behave like photons in the non-resonant low-frequency region, where a signal photon at THz frequency (ω_{THz}) and a near-IR idler photon (ω_i) are created simultaneously by a parametric process pumped with a near-IR pump photon (ω_p), according to the energy conservation law $\omega_p=\omega_{THz}+\omega_i$. In the stimulated scattering process, the momentum conservation law $\boldsymbol{k}_p = \boldsymbol{k}_i + \boldsymbol{k}_{THz}$ in noncollinear PM should be fulfilled. This leads to widely tunable THz wave and idler wave generation accomplished by changing the angle between the incident pump beam and idler beam. To enhance efficiency the idler wave is usually resonant in a cavity, known as THz parametric oscillation (TPO). THz parametric generation (TPG) is also feasible especially when a "seed" is injected for the idler wave without the resonant cavity, similar to optical parametric generation (OPG).

With similar advantages of wide tunability and high spectral purity, TPO and TPG demonstrate good potential applications in high-resolution spectroscopy and multispectral imaging [143]. Moreover, as their configuration is simpler than DFG with only one pump beam, it is more convenient to use

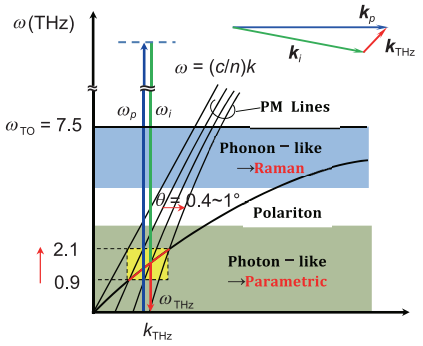

Figure 9 (Color online) Dispersion of the polariton and the principle of tunable THz generation due to the PM condition [142].

TPO/TPG sources than DFG sources in some cases combined with the pump probing technique [144], enabling the feasibility of high-sensitivity real-time imaging using near-IR array detectors.

4.1 TPO based on $LiNbO_3$

$LiNbO_3$ is one of the most suitable materials for generating THz waves through stimulated polariton scattering because of its large nonlinear coefficient [145] (d_{33}=25.2 pm/V at λ=1.064 μm) and its transparency over a wide wavelength range (0.4–5.5 μm). $LiNbO_3$ has four IR- and Raman-active transverse optical (TO) phonon modes, called A_1-symmetry modes, and the lowest mode (ω_0=248 cm^{-1}) is the most useful one for efficient tunable THz generation [146]. However, the absorption (10–100 cm^{-1}) and refractive index (around 5.2) of $LiNbO_3$ in the THz range is very large, and as a result, although strong THz waves can be generated inside the material, most of them are absorbed or totally reflected at the surface of the crystal. In the early works, specially prepared crystals with a proper cut angle were used to outcouple THz waves, avoiding total internal reflection (TIR) [147]. A grating structure on the surface of $LiNbO_3$ was also proposed to outcouple the THz wave directly to the free air space with almost one thousand times higher efficiency [148]. To improve the emitting characteristics, single Si-prism and arrayed Si-prism coupler were adopted (Figure 10(a)), greatly reducing the change of output direction variation during wavelength tuning [149,150].

Surface emission configuration (Figure 10(b)), in which the beam is emitted perpendicularly to the surface of the crystal, has considerable advantages because the THz-wave is extracted without any output coupler [151], and attenuation due to the short path length within the $LiNbO_3$ crystal is very low. We have made much effort on improving the output energy and tuning range of surface emitted TPOs. Li realized 0.87–2.73 THz tunable source with 9.12 μW average power corresponding to a conversion efficiency of 9.7×10^{-6}, pumped by a 10-Hz pulsed laser [152–154]. With a $LiNbO_3$ slab, Wang et al. [155] successfully obtained 3.56 times total

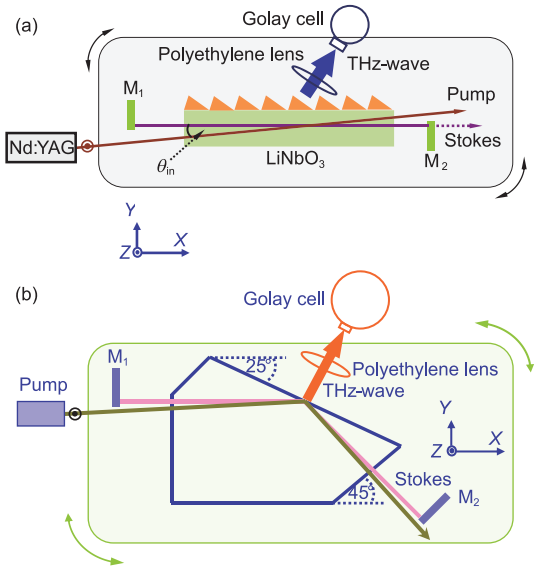

Figure 10 (Color online) $LiNbO_3$ based TPO with (a) arrayed Si-prism coupler and (b) surface-emission configuration.

THz power of a conventional surface-emitted TPO, in which the oscillating Stokes beams were totally reflected at the slab surface and propagated in a zigzagged path, emitting up to 5 THz beams perpendicularly to the crystal surface.

There are also some other techniques to lower the threshold and enhance the power for TPOs. Wu and Ikari [156] recycled the pump beam and increased the THz output almost four times in magnitude. Using longer nonlinear crystals to increase the gain or intracavity pumping in which the $LiNbO_3$ crystal is placed inside the laser cavity can make full use of the intracavity power and enable low threshold TPO. Edwards et al. [157] reported a low-threshold intracavity TPO with a quasi-CW diode pumped Nd:YAG laser, and the down-conversion efficiency at twice threshold reached close to 50%. Lee and Pask [158] realized CW THz generation in a bulk $LiNbO_3$ intracavity pumped by a diode-end-pumped Nd:$GdVO_4$ laser, giving 2.3 μW output power with 5.9 W incident diode pump power. They also observed cascaded stimulated polariton scattering and discussed the potential enhancement of THz output from cascading [159]. PPLN, which has much higher gain using QPM, is a better approach for lower threshold and higher conversion efficiency, with which low-peak-power quasi-CW or CW operation under various schemes have been investigated [160,161]. External cavity enhancement, which has been introduced in 3.6, is also an efficient method for TPO. Kiessling et al. [162] realized CW TPO based on PPLN with an enhancement cavity with a finesse of 500, giving tunable ranges from 1.2 to 2.9 THz at output power levels from 0.3 and 3.9 μW.

As we know, the output THz frequency is tuned by the angle between resonant idler wave and pump direction. However, for a fixed pump laser, tuning the whole TPO resonant cavity is sophisticated and slow. Fast frequency tuning through a special optical design, including a variable-angle mirror and an alignment telescope is feasible [163]. Minamide et al. [164] demonstrated a frequency-agile TPO in a ring-cavity configuration, in which a novel fast frequency-tuning method was realized by controlling a mirror of the three-mirror ring cavity. Recently, Yang et al. [165] achieved 12.9 μJ high-pulse-energy at 1.359 THz with a fast-tuning surface emitted ring-cavity configuration, enabled by a high-speed optical scanner.

4.2 Injection seeded narrow linewidth THz generation

Compared with TPO, the setup of TPG is simpler because it does not need a resonator. However, the efficiency of a TPG is usually very low, similar to OPG. Injection seeding, which uses a single-frequency laser working as the seed at the beginning of a pulse buildup period, makes the TPG both efficient and narrow linewidth. Fourier-transform limit TPG ($\Delta\nu$ <200 MHz) has been investigated since 2001 [166]. Guo et al. [167] reported an all-solid-state, narrow linewidth and wavelength-agile THz-wave parametric generator which could be rapidly and smoothly tuned over the range from 0.6 to 2.4 THz with a narrow linewidth of 50 MHz. Hayashi et al. [168] enhanced the tunability to 0.9–3 THz with high-intensity pumping from a subnanosecond microchip Nd:YAG laser. Tang et al. [169] also exploited the Stokes-pulse of a TPO and used it as the seeder to a TPG, greatly improving the output THz pulse energy. Injection seeding was also used in TPOs [170,171], but seeding into a cavity was much more complicated because of the seeding angle, despite of requiring the precise control of wavelength and cavity length for efficient resonation.

4.3 Picosecond THz parametric source

Most of the THz parametric sources reported up to now are pumped with nanosecond lasers, with a conversion efficiency from IR to THz wave of less than 10^{-7}. In 2015, Hayashi et al. [172] studied the SRS and SBS gains of a SPS process with nanosecond pump pulses, indicating that SBS had 1000 times larger gain than the SRS and concluded that for efficient frequency conversion, the duration of the pumping beam should be less than 1 ns. With a single-mode microchip Nd:YAG laser (20 mJ pulse energy, 420 ps pulse duration, 48 MW peak power) and a seeder (800 mW CW power), a 0.7–3 THz tunable THz source with an impressive output power (50 kW peak power, 0.2 GW/sr cm^2) was achieved, bringing the conversion efficiency to 2×10^{-4}. In the earlier studies, Takida et al. [173,174] reported 0.9–3.3 THz tunable TPOs synchronously pumped by 1.5 ps mode-locked Ti:sapphire lasers and a pump-enhanced cavity, owning the advantages of high repetition rate and good pulse-to-pulse stability for spectroscopy and imaging. Wu et al. [175] compared the THz parametric generation and amplification in different nonlinear materials pumped with a 520 ps passively

Q-switched Nd:YAG microchip laser at 1064 nm, achieving 5-W THz peak power and 22% pump depletion. Warrier et al. [176] demonstrated narrowband tunable THz generation with a $LiNbO_3$ crystal pumped by a CW mode-locked Nd:YVO_4 laser (15 ps, 80 MHz, 5.5 W), giving a 0.51–2.12 THz tuning range with etalon tuning and the output powers reached 3.7 μW at 1.6 THz and 2.4 μW at 0.9 THz, respectively. Picosecond lasers demonstrate superior characteristic in pumping for high-power THz generation, both suppressing the unnecessary SBS gain and increasing the damage threshold.

4.4 THz parametric source based on KTP and its isomorphs

Nonlinear crystals like KTP and its isomorphs (KTA, RTP etc.) exhibit excellent physical and optical characteristics and are widely used in OPO, SHG, etc. Interestingly, these crystals have a lot of TO phonon modes which are both IR and Raman active, making them feasible for THz parametric sources. The first report of a KTP TPO pumped by a pulsed Nd:YAG laser was presented in 2014 [177], owning three separated tuning bands of 3.17–3.44, 4.19–5.19 and 5.55–6.13 THz. Although the total tuning ranges were not impressive, it provided a solution for high-frequency THz source above 3 THz, far beyond the reach of $LiNbO_3$-based TPOs. A similar experiment was performed with KTA crystals using both the conventional Si-prism coupling and surface-emitted configuration [178]. In the experimental comparison with congruent-grown Mg:$LiNbO_3$, $LiNbO_3$ and $LiTaO_3$ under the same condition, KTP demonstrated superior FOM on SPS and higher THz power was observed [175]. Ortega et al. [179] reported a high-power, frequency-tunable RTP-based THz source emitting 16.2 μW average power at 3.8 THz intracavity pumped by a Q-switched Nd:YAG laser. To furtherly expand the tunability, we studied the PM characteristics of pumping with shorter wavelengths and conducted experiments on 532-nm-pumped KTP TPO [180], with which much wider tuning ranges covering 5.7–6.1, 7.4–7.8, 11.5–11.8 and 13.3–13.5 THz were obtained, successfully extending the TPO frequency range to over 10 THz.

5 Photomixing

Photomixing is a technique to generate widely-tunable CW or quasi-CW THz radiation through optical heterodyne down conversion, which shares several essential features at the fundamental level with THz photoconductive emitters discussed in Section 2.1. Composed of a high-speed photoconductor connected to a THz antenna on a photo-absorbing semiconductor substrate, the photomixer can convert two incident optical pump beams with a THz frequency difference into THz radiation. A commonly used antenna structure for photomixing is the logarithmic uniplanar spiral antenna (log-spiral antenna) with interdigitated electrode fingers, shown in Figure 11 [181]. The beat between two CW laser beams with slightly different frequencies ω_1 and ω_2, is excited and radiates as THz wave. The optical field at the antenna is the superposition of two input fields, expressed as [9]

$$E_{\text{opt}}(t) = E_1 e^{-i\omega_1 t} + E_2 e^{-i\omega_2 t}. \tag{11}$$

Thus, the optical intensity is given by

$$I_{\text{opt}}(t) = \frac{1}{2} c\varepsilon_0 \left| E_{\text{opt}}(t) \right|^2 = I_0 + I_{\text{B}} \cos(\omega_{\text{THz}} t), \tag{12}$$

where $I_0 = I_1 + I_2$ is the average pump intensity, $I_{\text{B}} = 2\sqrt{I_1 I_2}$ is the beat intensity, and $\omega_{\text{THz}} = \omega_1 - \omega_2$ is the difference frequency, extracted by the antenna into CW electromagnetic wave through the photocurrent induced dipole oscillation. Since currently available optical sources have broad frequency tunability, photomixers can generate THz waves over a wide frequency range by tuning the frequency difference between the optical pump beams. Moreover, photomixers can offer higher optical-to-THz conversion efficiencies since they are not constrained by the Manley-Rowe limit, compared with other photonic THz sources.

The photoconductive antenna is the key part of the THz photomixer [9,182]. The main challenge for a photomixer is the limited performance caused by the poor quantum efficiency of the high-speed photoconductors due to inefficient drift of photocarriers to the device contact electrodes within a fraction of THz radiation cycle. At the expense of a broad tuning range, the log-spiral antenna has low output power due to the relatively low radiation resistance. To enhance the THz output power, resonant antenna structures and more sophisticated antenna designs can be used to improve the carrier lifetime [183,184]. The other methods, for example, using a large excitation area and illuminating with an extended beam from a high-power laser are also noteworthy. A travelling-wave photomixer contains a long, thin active area

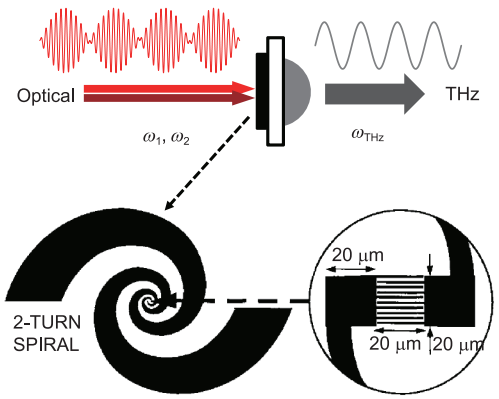

Figure 11 (Color online) (a) Schematic diagram of photomixing and (b) the log-spiral antenna with interdigitated electrode fingers [181].

between two electrodes, structured to maintain the coherent superposition between photocurrent and THz radiation [185]. Another approach to enhance photocurrent is to replace the prevailing LT-GaAs substrates with semiconductor heterostructures such as p-i-n photodiodes, overcoming the limiting factors for operation at high frequencies around 1 THz [182].

Plasmonic nanostructured antennas have been proved to be very effective in enhancing the quantum efficiency of photoconductive THz optoelectronics due to the unique capability of plasmonic contact electrodes in confining the incident optical pump beam in close proximity to the contact electrodes. Novel materials are also developed to achieve photomixing with high-performance telecommunication wavelengths obtained from high-power, wide-tunability, narrow-linewidth and compact semiconductor and fiber lasers. Recently, a plasmonic photomixer with plasmonic contact electrode gratings was fabricated on a ErAs:InGaAs substrate and characterized at 1550 nm pump wavelength, giving an order of magnitude enhancement in the 0.25–2.5 THz range compared with an analogous conventional photomixer without plasmonic contact electrodes [186]. GaAs plasmonic photomixers offering high THz power (17 μW) at 1 THz and wide tuning range of more than 2 THz were also presented [187]. Under lower duty cycles (2%), milliwatt level at 1 THz was obtained with a 1550 nm plasmonic photomixer [188].

Although the performance of photomixers is still limited, higher THz powers can be obtained through photomixer arrays and three-dimensional plasmonic contact electrodes to meet the requirements of higher THz powers and optical-to-THz conversion efficiencies [182]. These newly developed techniques, materials and antennas structures are promoting THz photomixers towards practical applications. Compared with the other photonic THz sources, photomixers are regarded as one of the most promising THz generation techniques for future compact and low-cost spectroscopic and communication systems with the advantages of excellent tunability, high spectral purity, room-temperature and on-chip operation.

6 Optically pumped gas lasers

The basic principle of optically pumped gas THz lasers are similar to typical laser systems based on population inversion in the active media, excited by external pumping sources. Gas molecules possessing large permanent dipole moments (>0.1 Debye) display a strong rotational transition spectrum in THz region. When such molecules are optically pumped by a shorter wavelength into a rotational level of a nearly empty vibrational state at low pressure, laser transitions in the excited vibrational state are possible. The basic concept is shown in Figure 12.

Optically pumped gas lasers provide powerful narrow-

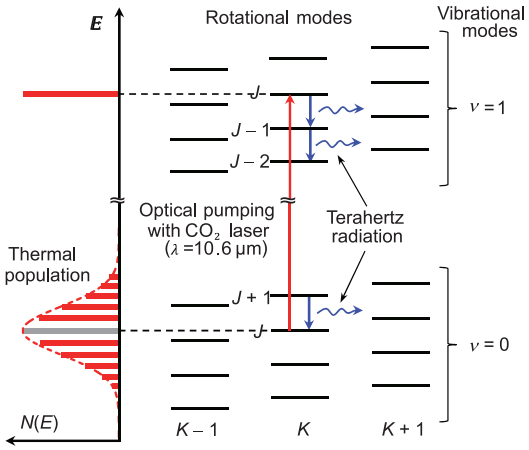

Figure 12 (Color online) Energy level diagram of optical excitation and THz radiation in an optically pumped THz gas laser.

linewidth THz radiation either in pulsed or CW mode. Various gain media for THz gas laser have been exploited since the 1970s [189–191], such as CH_3F, CH_3OH, NH_3, COOH, and CH_2F_2, giving thousands of THz lines in the 0.1–8 THz range. Some new materials containing isotopic elements of the conventional media were also researched for new THz lines [192]. Pumped by single-line high-power CO_2 lasers in the range of 9–11 μm, the pump-to-THz conversion efficiency can be very high (10^{-2}–10^{-3}) for high-power THz sources and commercial THz gas lasers over 100 mW are now available (https://www.edinst.com/products/firl-100-pumped-fir-system/). Although they are not continuously tunable, their high power and good brightness have enabled wide applications covering interferometry, polarimetry, scanning imaging, security inspection, radar modelling, etc.

The main disadvantage of optically pumped THz gas lasers is the large size due to the bulky CO_2 laser and the long gas cell for enough gain. To overcome these problems, some measures have been taken recently. Pagies et al. [193] demonstrated a low-threshold, relatively compact NH_3 gas laser pumped with a solid-state source—a quantum cascaded laser (QCL) around 10.3 μm, giving tens of microwatts THz power at 1.07 THz. Hollow-core optical fibers and photonic crystal fibers (PCFs), which are light, flexible and show low confinement loss, have been also theoretically investigated working as the reaction gas cell, showing the possibility of more compact THz gas lasers [194,195].

7 Conclusion

This paper gives a review on optically pumped THz sources, that is, THz sources excited by lasers, in both basic principles and developments. All kinds of operating modes from ultrafast, Q-switched to CW are included, covering but not limited within the whole THz range of 0.1–10 THz. However,

only the mainstream devices are elaborated. Some electrically pumped THz laser sources like QCLs and p-germanium lasers are not discussed here. Most of these optically pumped THz sources are good at frequency expanding (wideband or widely tunable) and are attractive for spectroscopy, imaging, communication and radar applications. It is noteworthy that the classical THz sources never stop making progress while the cutting-edge techniques are emerging in an endless stream and moving on quickly. These THz sources provide us powerful tools to investigate and change the world from various aspects. It is expected that this review will be helpful to researchers from all related areas and in turn to push the development of optically pump THz sources.

This work was supported by the National Basic Research Program of China (Grant No. 2014CB339802) and the National Natural Science Foundation of China (Grant Nos. 61675146, 61471257, 61505089, 61275102 & 61271066).

1 Tonouchi M. Cutting-edge terahertz technology. Nat Photon, 2007, 1: 97–105
2 Hosako I, Sekine N, Patrashin M, et al. At the dawn of a new era in terahertz technology. Proc IEEE, 2007, 95: 1611–1623
3 Nagatsuma T. Terahertz technologies: Present and future. IEICE Electron Express, 2011, 8: 1127–1142
4 Lewis R A. A review of terahertz sources. J Phys D-Appl Phys, 2014, 47: 374001
5 Williams G P. Filling the THz gap—high power sources and applications. Rep Prog Phys, 2006, 69: 301–326
6 Shumyatsky P, Alfano R R. Terahertz sources. J Biomed Opt, 2011, 16: 033001
7 Hoffmann M C, Fülöp J A. Intense ultrashort terahertz pulses: Generation and applications. J Phys D-Appl Phys, 2011, 44: 083001
8 Ding Y J. Progress in terahertz sources based on difference-frequency generation [Invited]. J Opt Soc Am B, 2014, 31: 2696–2711
9 Lee Y S. Principles of Terahertz Science and Technology. New York: Springer Science & Business Media, 2009
10 Grischkowsky D R, Keiding S R, van Exter M P, et al. Far-infrared time-domain spectroscopy with terahertz beams of dielectrics and semiconductors. J Opt Soc Am B, 1990, 7: 2006–2015
11 Hu B B, Nuss M C. Imaging with terahertz waves. Opt Lett, 1995, 20: 1716–1718
12 Fattinger C, Grischkowsky D. Terahertz beams. Appl Phys Lett, 1989, 54: 490–492
13 Auston D H, Cheung K P, Valdmanis J A, et al. Cherenkov radiation from femtosecond optical pulses in electro-optic media. Phys Rev Lett, 1984, 53: 1555–1558
14 Dai J, Xie X, Zhang X C. Detection of broadband terahertz waves with a laser-induced plasma in gases. Phys Rev Lett, 2006, 97: 103903
15 Zhang X C, Hu B B, Darrow J T, et al. Generation of femtosecond electromagnetic pulses from semiconductor surfaces. Appl Phys Lett, 1990, 56: 1011–1013
16 Auston D H, Smith P R. Generation and detection of millimeter waves by picosecond photoconductivity. Appl Phys Lett, 1983, 43: 631–633
17 Loka H S, Benjamin S D, Smith P W E. Optical characterization of low-temperature-grown GaAs for ultrafast all-optical switching devices. IEEE J Quantum Electron, 1998, 34: 1426–1437
18 Gregory I S, Baker C, Tribe W R, et al. High resistivity annealed low-temperature GaAs with 100 fs lifetimes. Appl Phys Lett, 2003, 83: 4199–4201
19 Sartorius B, Roehle H, Künzel H, et al. All-fiber terahertz time-domain spectrometer operating at 1.5 μm telecom wavelengths. Opt Express, 2008, 16: 9565–9570
20 Globisch B, Dietz R J B, Kohlhaas R B, et al. Fiber-coupled transceiver for terahertz reflection measurements with a 45 THz bandwidth. Opt Lett, 2016, 41: 5262–5265
21 You D, Jones R R, Bucksbaum P H, et al. Generation of high-power sub-single-cycle 500-fs electromagnetic pulses. Opt Lett, 1993, 18: 290–292
22 Budiarto E, Margolies J, Jeong S, et al. High-intensity terahertz pulses at 1-kHz repetition rate. IEEE J Quantum Electron, 1996, 32: 1839–1846
23 Beck M, Schäfer H, Klatt G, et al. Impulsive terahertz radiation with high electric fields from an amplifier-driven large-area photoconductive antenna. Opt Express, 2010, 18: 9251–9257
24 Park S G, Jin K H, Yi M, et al. Enhancement of terahertz pulse emission by optical nanoantenna. ACS Nano, 2012, 6: 2026–2031
25 Yang S H, Hashemi M R, Berry C W, et al. 7.5% Optical-to-terahertz conversion efficiency offered by photoconductive emitters with three-dimensional plasmonic contact electrodes. IEEE Trans THz Sci Technol, 2014, 4: 575–581
26 Ropagnol X, Khorasaninejad M, Raeiszadeh M, et al. Intense THz pulses with large ponderomotive potential generated from large aperture photoconductive antennas. Opt Express, 2016, 24: 11299–11311
27 Bass M, Franken P A, Ward J F, et al. Optical rectification. Phys Rev Lett, 1962, 9: 446–448
28 Yang K H, Richards P L, Shen Y R. Generation of far-infrared radiation by picosecond light pulses in $LiNbO_3$. Appl Phys Lett, 1971, 19: 320–323
29 Vodopyanov K L. Optical generation of narrow-band terahertz packets in periodically-inverted electro-optic crystals: Conversion efficiency and optimal laser pulse format. Opt Express, 2006, 14: 2263–2276
30 Sutherland R L. Handbook of Nonlinear Optics. New York: CRC Press, 2003
31 Nahata A, Weling A S, Heinz T F. A wideband coherent terahertz spectroscopy system using optical rectification and electro-optic sampling. Appl Phys Lett, 1996, 69: 2321–2323
32 Chang G, Divin C J, Liu C H, et al. Power scalable compact THz system based on an ultrafast Yb-doped fiber amplifier. Opt Express, 2006, 14: 7909–7913
33 Nagai M, Tanaka K, Ohtake H, et al. Generation and detection of terahertz radiation by electro-optical process in GaAs using 1.56 μm fiber laser pulses. Appl Phys Lett, 2004, 85: 3974–3976
34 Vodopyanov K L, Fejer M M, Yu X, et al. Terahertz-wave generation in quasi-phase-matched GaAs. Appl Phys Lett, 2006, 89: 141119
35 Hebling J, Almasi G, Kozma I Z, et al. Velocity matching by pulse front tilting for large area THz-pulse generation. Opt Express, 2002, 10: 1161–1166
36 Huang S W, Granados E, Huang W R, et al. High conversion efficiency, high energy terahertz pulses by optical rectification in cryogenically cooled lithium niobate. Opt Lett, 2013, 38: 796–798
37 Fülöp J A, Ollmann Z, Lombosi C, et al. Efficient generation of THz pulses with 04 mJ energy. Opt Express, 2014, 22: 20155–20163
38 Zhong S C, Li J, Zhai Z H, et al. Generation of 019-mJ THz pulses in $LiNbO_3$ driven by 800-nm femtosecond laser. Opt Express, 2016, 24: 14828–14835
39 Askar'Yan G A. Cherenkov radiation and transition radiation from electromagnetic waves. Sov Phys JETP, 1962, 37: 594–596
40 Auston D H. Subpicosecond electro-optic shock waves. Appl Phys Lett, 1983, 43: 713–715
41 Kleinman D A, Auston D H. Theory of electrooptic shock radiation in nonlinear optical media. IEEE J Quantum Electron, 1984, 20: 964–970

42 Stepanov A G, Hebling J, Kuhl J. THz generation via optical rectification with ultrashort laser pulse focused to a line. Appl Phys B, 2005, 81: 23–26
43 Stepanov A G, Kuhl J, Kozma I Z, et al. Scaling up the energy of THz pulses created by optical rectification. Opt Express, 2005, 13: 5762–5768
44 Bodrov S B, Stepanov A N, Bakunov M I, et al. Highly efficient optical-to-terahertz conversion in a sandwich structure with $LiNbO_3$ core. Opt Express, 2009, 17: 1871–1879
45 Takeya K, Minami T, Okano H, et al. Enhanced Cherenkov phase matching terahertz wave generation via a magnesium oxide doped lithium niobate ridged waveguide crystal. APL Photonics, 2017, 2: 016102
46 Liu P, Xu D, Liu C, et al. p-Polarized Cherenkov THz wave radiation generated by optical rectification for a Brewster-cut $LiNbO_3$ crystal. J Opt, 2011, 13: 085202
47 Clough B, Dai J, Zhang X C. Laser air photonics: Beyond the terahertz gap. Mater Today, 2012, 15: 50–58
48 Hafez H A, Chai X, Ibrahim A, et al. Intense terahertz radiation and their applications. J Opt, 2016, 18: 093004
49 Hamster H, Sullivan A, Gordon S, et al. Subpicosecond, electromagnetic pulses from intense laser-plasma interaction. Phys Rev Lett, 1993, 71: 2725–2728
50 Cook D J, Hochstrasser R M. Intense terahertz pulses by four-wave rectification in air. Opt Lett, 2000, 25: 1210–1212
51 Kim K Y, Taylor A J, Glownia J H, et al. Coherent control of terahertz supercontinuum generation in ultrafast laser-gas interactions. Nat Photon, 2008, 2: 605–609
52 Thomson M D, Blank V, Roskos H G. Terahertz white-light pulses from an air plasma photo-induced by incommensurate two-color optical fields. Opt Express, 2010, 18: 23173–23182
53 Matsubara E, Nagai M, Ashida M. Ultrabroadband coherent electric field from far infrared to 200 THz using air plasma induced by 10 fs pulses. Appl Phys Lett, 2012, 101: 011105
54 Kuk D, Yoo Y J, Rosenthal E W, et al. Generation of scalable terahertz radiation from cylindrically focused two-color laser pulses in air. Appl Phys Lett, 2016, 108: 121106
55 Kress M, Löffler T, Eden S, et al. Terahertz-pulse generation by photoionization of air with laser pulses composed of both fundamental and second-harmonic waves. Opt Lett, 2004, 29: 1120–1122
56 Kim K Y, Glownia J H, Taylor A J, et al. Terahertz emission from ultrafast ionizing air in symmetry-broken laser fields. Opt Express, 2007, 15: 4577–4584
57 Roskos H G, Thomson M D, Kreß M, et al. Broadband THz emission from gas plasmas induced by femtosecond optical pulses: From fundamentals to applications. Laser Photon Rev, 2007, 1: 349–368
58 Karpowicz N, Zhang X C. Coherent terahertz echo of tunnel ionization in gases. Phys Rev Lett, 2009, 102: 093001
59 Gildenburg V B, Vvedenskii N V. Optical-to-THz wave conversion via excitation of plasma oscillations in the tunneling-ionization process. Phys Rev Lett, 2007, 98: 245002
60 Vvedenskii N V, Korytin A I, Kostin V A, et al. Two-color laser-plasma generation of terahertz radiation using a frequency-tunable half harmonic of a femtosecond pulse. Phys Rev Lett, 2014, 112: 055004
61 Debayle A, Gremillet L, Bergé L, et al. Analytical model for THz emissions induced by laser-gas interaction. Opt Express, 2014, 22: 13691–13709
62 Li N, Bai Y, Miao T, et al. Revealing plasma oscillation in THz spectrum from laser plasma of molecular jet. Opt Express, 2016, 24: 23009–23017
63 Zernike F, Berman P R. Generation of far infrared as a difference frequency. Phys Rev Lett, 1965, 15: 999–1001
64 Faries D W, Gehring K A, Richards P L, et al. Tunable far-infrared radiation generated from the difference frequency between two ruby lasers. Phys Rev, 1969, 180: 363–365
65 Shi W, Ding Y J, Fernelius N, et al. Efficient, tunable, and coherent 018–527-THz source based on GaSe crystal. Opt Lett, 2002, 27: 1454–1456
66 Shi W, Ding Y J. Tunable coherent radiation from terahertz to microwave by mixing two infrared frequencies in a 47-MM-long GaSe crystal. Int J High Speed Electron Syst, 2006, 16: 589–595
67 Shi W, Ding Y J. A monochromatic and high-power terahertz source tunable in the ranges of 2.7–38.4 and 58.2–3540 μm for variety of potential applications. Appl Phys Lett, 2004, 84: 1635–1637
68 Shi W, Ding Y J. Generation of backward terahertz waves in GaSe crystals. Opt Lett, 2005, 30: 1861–1863
69 Jiang Y, Ding Y J. Generation of 260-μW Fourier-transform-limited nanosecond THz pulses by frequency-mixing two CO_2 lasers. In: Lasers and Electro-Optics and Conference on Quantum Electronics and Laser Science. San Jose: IEEE, 2008
70 Shi W, Leigh M A, Zong J, et al. High-power all-fiber-based narrow-linewidth single-mode fiber laser pulses in the C-band and frequency conversion to THz generation. IEEE J Sel Top Quantum Electron, 2009, 15: 377–384
71 Zhao P, Ragam S, Ding Y J, et al. Compact and portable terahertz source by mixing two frequencies generated simultaneously by a single solid-state laser. Opt Lett, 2010, 35: 3979–3981
72 Zhao P, Ragam S, Ding Y J, et al. Investigation of terahertz generation from passively Q-switched dual-frequency laser pulses. Opt Lett, 2011, 36: 4818–4820
73 Liu Y, Zhong K, Mei J, et al. Compact and flexible dual-wavelength laser generation in coaxial diode-end-pumped configuration. IEEE Photonics J, 2017, 9: 1–10
74 Zhong K, Yao J, Xu D, et al. Enhancement of terahertz wave difference frequency generation based on a compact walk-off compensated KTP OPO. Opt Commun, 2010, 283: 3520–3524
75 Mei J, Zhong K, Wang M, et al. Widely-tunable high-repetition-rate terahertz generation in GaSe with a compact dual-wavelength KTP OPO around 2 μm. Opt Express, 2016, 24: 23368–23375
76 Mei J, Zhong K, Wang M, et al. Compact and flexible dual-wavelength laser generation in coaxial diode-end-pumped configuration. IEEE Photonics J, 2016, 8: 5502107
77 Shi W, Ding Y J. Continuously tunable and coherent terahertz radiation by means of phase-matched difference-frequency generation in zinc germanium phosphide. Appl Phys Lett, 2003, 83: 848–850
78 Creeden D, McCarthy J C, Ketteridge P A, et al. Compact fiber-pumped terahertz source based on difference frequency mixing in ZGP. IEEE J Sel Top Quantum Electron, 2007, 13: 732–737
79 Zernike F. Temperature-dependent phase matching for far-infrared difference-frequency generation in InSb. Phys Rev Lett, 1969, 22: 931–933
80 Bridges T J, Strnad A R. Submillimeter wave generation by difference-frequency mixing in GaAs. Appl Phys Lett, 1972, 20: 382–384
81 Aggarwal R L, Lax B, Favrot G. Noncollinear phase matching in GaAs. Appl Phys Lett, 1973, 22: 329–330
82 Lee N, Lax B, Aggarwal R L. F3 high power far infrared generation in GaAs. Opt Commun, 1976, 18: 50–51
83 Tochitsky S Y, Ralph J E, Sung C, et al. Generation of megawatt-power terahertz pulses by noncollinear difference-frequency mixing in GaAs. J Appl Phys, 2005, 98: 026101–026101
84 Tochitsky S Y, Sung C, Trubnick S E, et al. High-power tunable, 05–3 THz radiation source based on nonlinear difference frequency mixing of CO_2 laser lines. J Opt Soc Am B, 2007, 24: 2509–2516
85 Tanabe T, Suto K, Nishizawa J, et al. Frequency-tunable high-power terahertz wave generation from GaP. J Appl Phys, 2003, 93: 4610–4615
86 Tanabe T, Suto K, Nishizawa J, et al. Tunable terahertz wave generation in the 3- to 7-THz region from GaP. Appl Phys Lett, 2003, 83: 237–239
87 Tanabe T, Suto K, Nishizawa J, et al. Frequency-tunable terahertz wave generation via excitation of phonon-polaritons in GaP. J Phys

D-Appl Phys, 2003, 36: 953–957
88 Armstrong J A, Bloembergen N, Ducuing J, et al. Interactions between light waves in a nonlinear dielectric. Phys Rev, 1962, 127: 1918–1939
89 Gordon L, Woods G L, Eckardt R C, et al. Diffusion-bonded stacked GaAs for quasiphase-matched second-harmonic generation of a carbon dioxide laser. Electron Lett, 1993, 29: 1942–1944
90 Myers L E, Eckardt R C, Fejer M M, et al. Quasi-phase-matched optical parametric oscillators in bulk periodically poled $LiNbO_3$. J Opt Soc Am B, 1995, 12: 2102–2116
91 Eyres L A, Tourreau P J, Pinguet T J, et al. All-epitaxial fabrication of thick, orientation-patterned GaAs films for nonlinear optical frequency conversion. Appl Phys Lett, 2001, 79: 904–906
92 Wang T D, Lin S T, Lin Y Y, et al. Forward and backward terahertz-wave difference-frequency generations from periodically poled lithium niobate. Opt Express, 2008, 16: 6471–6478
93 Sasaki Y, Yuri A, Kawase K, et al. Terahertz-wave surface-emitted difference frequency generation in slant-stripe-type periodically poled $LiNbO_3$ crystal. Appl Phys Lett, 2002, 81: 3323–3325
94 Scheller M, Yarborough J M, Moloney J V, et al. Room temperature continuous wave milliwatt terahertz source. Opt Express, 2010, 18: 27112–27117
95 Vodopyanov K L. Optical THz-wave generation with periodically-inverted GaAs. Laser Photon Rev, 2008, 2: 11–25
96 Jiang Y, Li D, Ding Y J, et al. Terahertz generation based on parametric conversion: From saturation of conversion efficiency to back conversion. Opt Lett, 2011, 36: 1608–1610
97 Zhao P, Ragam S, Ding Y J, et al. Terahertz intracavity generation from output coupler consisting of stacked GaP plates. Appl Phys Lett, 2012, 101: 021107
98 Petersen E B, Shi W, Chavez-Pirson A, et al. Efficient parametric terahertz generation in quasi-phase-matched GaP through cavity enhanced difference-frequency generation. Appl Phys Lett, 2011, 98: 121119
99 Schaar J E, Vodopyanov K L, Fejer M M. Intracavity terahertz-wave generation in a synchronously pumped optical parametric oscillator using quasi-phase-matched GaAs. Opt Lett, 2007, 32: 1284–1286
100 Kiessling J, Breunig I, Schunemann P G, et al. High power and spectral purity continuous-wave photonic THz source tunable from 1 to 4.5 THz for nonlinear molecular spectroscopy. New J Phys, 2013, 15: 105014
101 Liu P, Xu D, Jiang H, et al. Theory of monochromatic terahertz generation via Cherenkov phase-matched difference frequency generation in $LiNbO_3$ crystal. J Opt Soc Am B, 2012, 29: 2425–2430
102 Suizu K, Shibuya T, Akiba T, et al. Čherenkov phase-matched monochromatic THzwave generation using difference frequency generation with a lithium niobate crystal. Opt Express, 2008, 16: 7493–7498
103 Shibuya T, Tsutsui T, Suizu K, et al. Efficient cherenkov-type phase-matched widely tunable terahertz-wave generation via an optimized pump beam shape. Appl Phys Express, 2009, 2: 032302
104 Suizu K, Koketsu K, Shibuya T, et al. Extremely frequency-widened terahertz wave generation using Cherenkov-type radiation. Opt Express, 2009, 17: 6676–6681
105 Shibuya T, Suizu K, Kawase K. Widely tunable monochromatic Cherenkov phase-matched terahertz wave generation from bulk lithium niobate. Appl Phys Express, 2010, 3: 082201
106 Liu P, Xu D, Li J, et al. Monochromatic cherenkov thz source pumped by a singly resonant optical parametric oscillator. IEEE Photon Technol Lett, 2014, 26: 494–496
107 Suizu K, Miyamoto K, Yamashita T, et al. High-power terahertz-wave generation using DAST crystal and detection using mid-infrared powermeter. Opt Lett, 2007, 32: 2885–2887
108 Taniuchi T, Ikeda S, Mineno Y, et al. Terahertz properties of a new organic crystal, 4¢-dimethylamino-*N*-methyl-4-stilbazolium *p*-chlorobenzenesulfonate. Jap J Appl Phys, 2005, 44: L932–L934
109 Matsukawa T, Notake T, Nawata K, et al. Terahertz-wave generation from 4-dimethylamino-*N*¢-methyl-4¢-stilbazolium p-bromobenzenesulfonate crystal: Effect of halogen substitution in a counter benzenesulfonate of stilbazolium derivatives. Opt Mater, 2014, 36: 1995–1999
110 Miyamoto K, Ohno S, Fujiwara M, et al. Optimized terahertz-wave generation using BNA-DFG. Opt Express, 2009, 17: 14832–14838
111 Taniuchi T, Shikata J, Ito H. Tunable terahertz-wave generation in DAST crystal with dual-wavelength KTP optical parametric oscillator. Electron Lett, 2000, 36: 1414–1416
112 Ito H, Suizu K, Yamashita T, et al. Random frequency accessible broad tunable terahertz-wave source using phase-matched 4-dimethylamino-*N*-methyl-4-stilbazolium tosylate crystal. Jpn J Appl Phys, 2007, 46: 7321–7324
113 Liu J, Merkt F. Generation of tunable Fourier-transform-limited terahertz pulses in 4-*N*,*N*-dimethylamino-4¢-*N*¢-methyl stilbazolium tosylate crystals. Appl Phys Lett, 2008, 93: 131105
114 Zhong K, Mei J, Wang M, et al. Compact high-repetition-rate monochromatic terahertz source based on difference frequency generation from a dual-wavelength Nd:YAG laser and DAST crystal. J Infrared Milli Terahz Waves, 2017, 38: 87–95
115 Liu P, Xu D, Li Y, et al. Widely tunable and monochromatic terahertz difference frequency generation with organic crystal DSTMS. EPL, 2014, 106: 60001
116 Liu P, Zhang X, Yan C, et al. Widely tunable and monochromatic terahertz difference frequency generation with organic crystal 2-(3-(4-hydroxystyryl)-5,5-dime-thylcyclohex-2-enylidene) malononitrile. Appl Phys Lett, 2016, 108: 011104
117 Thompson D E, Coleman P D. Step-tunable far infrared radiation by phase matched mixing in planar-dielectric waveguides. IEEE Trans Microwave Theor Techn, 1974, 22: 995–1000
118 Marandi A, Darcie T E, So P P M. Design of a continuous-wave tunable terahertz source using waveguide-phase-matched GaAs. Opt Express, 2008, 16: 10427–10433
119 Vodopyanov K L, Avetisyan Y H. Optical terahertz wave generation in a planar GaAs waveguide. Opt Lett, 2008, 33: 2314–2316
120 Zangeneh H R, Jahromi M A F, Jahromi M A F. Design of a terahertz source using a nano-slot of GaAs. J Opt, 2014, 43: 173–176
121 Nishizawa J I, Suto K, Tanabe T, et al. THz generation from GaP rod-type waveguides. IEEE Photon Technol Lett, 2007, 19: 143–145
122 Saito K, Tanabe T, Oyama Y. Elliptically polarized THz-wave generation from GaP-THz planar waveguide via collinear phase-matched difference frequency mixing. Opt Express, 2012, 20: 26082–26088
123 Saito K, Tanabe T, Oyama Y. Widely tunable terahertz-wave generation from planar GaP waveguides via difference frequency generation under collinear phase-matching condition. Jpn J Appl Phys, 2014, 53: 102203
124 Cherchi M, Taormina A, Busacca A C, et al. Exploiting the optical quadratic nonlinearity of zinc-blende semiconductors for guided-wave terahertz generation: A material comparison. IEEE J Quantum Electron, 2010, 46: 368–376
125 Saito K, Tanabe T, Oyama Y. THz-wave generation via difference frequency mixing in strained silicon based waveguide utilizing its second order susceptibility $\chi^{(2)}$. Opt Express, 2014, 22: 16660–16668
126 Baehr-Jones T, Hochberg M, Soref R, et al. Design of a tunable, room temperature, continuous-wave terahertz source and detector using silicon waveguides. J Opt Soc Am B, 2008, 25: 261–268
127 Sinha R, Karabiyik M, Al-Amin C, et al. Tunable room temperature THz sources based on nonlinear mixing in a hybrid optical and THz micro-ring resonator. Sci Rep, 2015, 5: 9422
128 Ding Y J. Terahertz parametric converters by use of novel metallic-dielectric hybrid waveguides. J Opt Soc Am B, 2006, 23: 1354–1359
129 Liu P, Shi W, Xu D, et al. High-power high-brightness terahertz source based on nonlinear optical crystal fiber. IEEE J Sel Top Quantum Electron, 2016, 22: 360–364
130 Ashkin A, Boyd G, Dziedzic J. Resonant optical second harmonic

generation and mixing. IEEE J Quantum Electron, 1966, 2: 109–124
131 Theuer M, Molter D, Maki K, et al. Terahertz generation in an actively controlled femtosecond enhancement cavity. Appl Phys Lett, 2008, 93: 041119
132 Tanaka R, Matsuzawa T, Yokota H, et al. Stable confinement of nanosecond laser pulse in an enhancement cavity. Opt Express, 2008, 16: 18667–18674
133 Kozlovsky W J, Nabors C D, Byer R L. Efficient second harmonic generation of a diode-laser-pumped CW Nd:YAG laser using monolithic MgO:$LiNbO_3$ external resonant cavities. IEEE J Quantum Electron, 1988, 24: 913–919
134 Petersen E B, Shi W, Nguyen D T, et al. Enhanced terahertz source based on external cavity difference-frequency generation using monolithic single-frequency pulsed fiber lasers. Opt Lett, 2010, 35: 2170–2172
135 Paul J R, Scheller M, Laurain A, et al. Narrow linewidth single-frequency terahertz source based on difference frequency generation of vertical-external-cavity source-emitting lasers in an external resonance cavity. Opt Lett, 2013, 38: 3654–3657
136 Cronin-Golomb M. Cascaded nonlinear difference-frequency generation of enhanced terahertz wave production. Opt Lett, 2004, 29: 2046–2048
137 Schaar J E, Vodopyanov K L, Kuo P S, et al. Terahertz sources based on intracavity parametric down-conversion in quasi-phase-matched gallium arsenide. IEEE J Sel Top Quantum Electron, 2008, 14: 354–362
138 Zhong K, Yao J Q, Xu D G, et al. Theoretical research on cascaded difference frequency generation of terahertz radiation (in Chinese). Acta Phys Sin, 2011, 60: 034210
139 Hu C F, Zhong K, Mei J L, et al. Theoretical analysis of terahertz generation in periodically inverted nonlinear crystals based on cascaded difference frequency generation process. Mod Phys Lett B, 2015, 29: 1450263
140 Liu P, Xu D, Yu H, et al. Coupled-mode theory for cherenkov-type guided-wave terahertz generation via cascaded difference frequency generation. J Lightwave Technol, 2013, 31: 2508–2514
141 Ravi K, Hemmer M, Cirmi G, et al. Cascaded parametric amplification for highly efficient terahertz generation. Opt Lett, 2016, 41: 3806–3809
142 Hayashi S, Nawata K, Sakai H, et al. High-power, single-longitudinal-mode terahertz-wave generation pumped by a microchip Nd:YAG laser [Invited]. Opt Express, 2012, 20: 2881–2886
143 Dobroiu A, Otani C, Kawase K. Terahertz-wave sources and imaging applications. Meas Sci Technol, 2006, 17: R161–R174
144 Guo R, Ikar'i T, Zhang J, et al. Frequency-agile THz-wave generation and detection system using nonlinear frequency conversion at room temperature. Opt Express, 2010, 18: 16430–16436
145 Shoji I, Kondo T, Kitamoto A, et al. Absolute scale of second-order nonlinear-optical coefficients. J Opt Soc Am B, 1997, 14: 2268–2294
146 Shikata J, Kawase K, Karino K, et al. Tunable terahertz-wave parametric oscillators using $LiNbO_3$ and MgO:$LiNbO_3$ crystals. IEEE Trans Microwave Theor Techn, 2000, 48: 653–661
147 Johnson B C, Puthoff H E, SooHoo J, et al. Power and linewidth of tunable stimulated far-infrared emission in $LiNbO_3$. Appl Phys Lett, 1971, 18: 181–183
148 Kawase K, Sato M, Taniuchi T, et al. Coherent tunable THz-wave generation from $LiNbO_3$ with monolithic grating coupler. Appl Phys Lett, 1996, 68: 2483–2485
149 Kawase K, Sato M, Nakamura K, et al. Unidirectional radiation of widely tunable THz wave using a prism coupler under noncollinear phase matching condition. Appl Phys Lett, 1997, 71: 753–755
150 Kawase K, Shikata J I, Minamide H, et al. Arrayed silicon prism coupler for a terahertz-wave parametric oscillator. Appl Opt, 2001, 40: 1423–1426
151 Ikari T, Zhang X, Minamide H, et al. THz-wave parametric oscillator with a surface-emitted configuration. Opt Express, 2006, 14: 1604–1610
152 Li Z Y, Yao J Q, Xu D G, et al. High-power terahertz radiation from surface-emitted THz-wave parametric oscillator. Chin Phys B, 2011, 20: 054207
153 Li Z Y, Yao J Q, Xu D G, et al. Output enhancement of a THz wave based on a surface-emitted THz-wave parametric oscillator. Chin Phys Lett, 2011, 28: 114201
154 Li Z, Bing P, Yao J, et al. High-powered tunable terahertz source based on a surface-emitted terahertz-wave parametric oscillator. Opt Eng, 2012, 51: 091605
155 Wang W, Zhang X, Wang Q, et al. Multiple-beam output of a surface-emitted terahertz-wave parametric oscillator by using a slab MgO:$LiNbO_3$ crystal. Opt Lett, 2014, 39: 754–757
156 Wu D H, Ikari T. Enhancement of the output power of a terahertz parametric oscillator with recycled pump beam. Appl Phys Lett, 2009, 95: 141105
157 Edwards T, Walsh D, Spurr M, et al. Compact source of continuously and widely-tunable terahertz radiation. Opt Express, 2006, 14: 1582–1589
158 Lee A J, Pask H M. Continuous wave, frequency-tunable terahertz laser radiation generated via stimulated polariton scattering. Opt Lett, 2014, 39: 442–445
159 Lee A J, Pask H M. Cascaded stimulated polariton scattering in a Mg:$LiNbO_3$ terahertz laser. Opt Express, 2015, 23: 8687–8698
160 Sowade R, Breunig I, Cámara Mayorga I, et al. Continuous-wave optical parametric terahertz source. Opt Express, 2009, 17: 22303–22310
161 Molter D, Theuer M, Beigang R. Nanosecond terahertz optical parametric oscillator with a novel quasi phase matching scheme in lithium niobate. Opt Express, 2009, 17: 6623–6628
162 Kiessling J, Fuchs F, Buse K, et al. Pump-enhanced optical parametric oscillator generating continuous wave tunable terahertz radiation. Opt Lett, 2011, 36: 4374–4376
163 Imai K, Kawase K, Ito H. A frequency-agile terahertz-wave parametric oscillator. Opt Express, 2001, 8: 699–704
164 Minamide H, Ikari T, Ito H. Frequency-agile terahertz-wave parametric oscillator in a ring-cavity configuration. Rev Sci Instrum, 2009, 80: 123104–123104
165 Yang Z, Wang Y, Xu D, et al. High-energy terahertz wave parametric oscillator with a surface-emitted ring-cavity configuration. Opt Lett, 2016, 41: 2262
166 Kawase K, Shikata J, Imai K, et al. Transform-limited, narrow-linewidth, terahertz-wave parametric generator. Appl Phys Lett, 2001, 78: 2819–2821
167 Guo R, Akiyama K, Minamide H, et al. All-solid-state, narrow linewidth, wavelength-agile terahertz-wave generator. Appl Phys Lett, 2006, 88: 091120
168 Hayashi S, Shibuya T, Sakai H, et al. Tunability enhancement of a terahertz-wave parametric generator pumped by a microchip Nd:YAG laser. Appl Opt, 2009, 48: 2899–2902
169 Tang G, Cong Z, Qin Z, et al. Energy scaling of terahertz-wave parametric sources. Opt Express, 2015, 23: 4144–4152
170 Imai K, Kawase K, Shikata J, et al. Injection-seeded terahertz-wave parametric oscillator. Appl Phys Lett, 2001, 78: 1026–1028
171 Walsh D, Stothard D J M, Edwards T J, et al. Injection-seeded intracavity terahertz optical parametric oscillator. J Opt Soc Am B, 2009, 26: 1196–1202
172 Hayashi S, Nawata K, Taira T, et al. Ultrabright continuously tunable terahertz-wave generation at room temperature. Sci Rep, 2015, 4: 5045
173 Takida Y, Maeda S, Ohira T, et al. Noncascading THz-wave parametric oscillator synchronously pumped by mode-locked picosecond Ti:sapphire laser in doubly-resonant external cavity. Opt Commun, 2011, 284: 4663–4666
174 Takida Y, Ohira T, Tadokoro Y, et al. Tunable picosecond terahertz-wave parametric oscillators based on noncollinear pump-enhanced

signal-resonant cavity. IEEE J Sel Top Quantum Electron, 2013, 19: 8500307–8500307
175 Wu M H, Chiu Y C, Wang T D, et al. Terahertz parametric generation and amplification from potassium titanyl phosphate in comparison with lithium niobate and lithium tantalate. Opt Express, 2016, 24: 25964–25973
176 Warrier A M, Li R, Lin J, et al. Tunable terahertz generation in the picosecond regime from the stimulated polariton scattering in a $LiNbO_3$ crystal. Opt Lett, 2016, 41: 4409–4412
177 Wang W, Cong Z, Chen X, et al. Terahertz parametric oscillator based on $KTiOPO_4$ crystal. Opt Lett, 2014, 39: 3706–3709
178 Wang W, Cong Z, Liu Z, et al. THz-wave generation via stimulated polariton scattering in $KTiOAsO_4$ crystal. Opt Express, 2014, 22: 17092–17098
179 Ortega T A, Pask H M, Spence D J, et al. Stimulated polariton scattering in an intracavity $RbTiOPO_4$ crystal generating frequency-tunable THz output. Opt Express, 2016, 24: 10254–10264
180 Yan C, Wang Y, Xu D, et al. Green laser induced terahertz tuning range expanding in $KTiOPO_4$ terahertz parametric oscillator. Appl Phys Lett, 2016, 108: 011107
181 Verghese S, McIntosh K A, Brown E R. Highly tunable fiber-coupled photomixers with coherent terahertz output power. IEEE Trans Microwave Theor Techn, 1997, 45: 1301–1309
182 Preu S, Döhler G H, Malzer S, et al. Tunable, continuous-wave terahertz photomixer sources and applications. J Appl Phys, 2011, 109: 061301–061301
183 Matsuura S, Tani M, Sakai K. Generation of coherent terahertz radiation by photomixing in dipole photoconductive antennas. Appl Phys Lett, 1997, 70: 559–561
184 Duffy S M, Verghese S, McIntosh A, et al. Accurate modeling of dual dipole and slot elements used with photomixers for coherent terahertz output power. IEEE Trans Microwave Theor Techn, 2001, 49: 1032–1038
185 Sakai K. Terahertz Optoelectronics. Berlin: Springer, 2005
186 Berry C W, Hashemi M R, Preu S, et al. Plasmonics enhanced photomixing for generating quasi-continuous-wave frequency-tunable terahertz radiation. Opt Lett, 2014, 39: 4522–4524
187 Yang S H, Jarrahi M. Frequency-tunable continuous-wave terahertz sources based on GaAs plasmonic photomixers. Appl Phys Lett, 2015, 107: 131111
188 Berry C W, Hashemi M R, Preu S, et al. High power terahertz generation using 1550 nm plasmonic photomixers. Appl Phys Lett, 2014, 105: 011121
189 Chantry G W. Long-Wave Optics: the Science and Technology of Infrared and Near-Millimetre Waves. London: Academic Press, 1984
190 Mukhopadhyay I, Singh S. Optically pumped far infrared molecular lasers: Molecular and application aspects. Spectrochim Acta Part A-Mol Biomolec Spectr, 1998, 54: 395–410
191 Dodel G. On the history of far-infrared (FIR) gas lasers: Thirty-five years of research and application. Infrared Phys Tech, 1999, 40: 127–139
192 McKnight M, Penoyar P, Pruett M, et al. New far-infrared laser emissions from optically pumped CH_2DOH, CHD_2OH, and $CH_3{}^{18}OH$. IEEE J Quantum Electron, 2014, 50: 42–46
193 Pagies A, Ducournau G, Lampin J F. Continuous wave terahertz molecular laser optically pumped by a quantum cascade laser. In: 41st International Conference on Infrared, Millimeter, and Terahertz waves (IRMMW-THz). Copenhagen: IEEE, 2016. 1–2
194 Nampoothiri A V V, Jones A M, Fourcade-Dutin C, et al. Hollow-core optical fiber gas lasers (HOFGLAS): A review [Invited]. Opt Mater Express, 2012, 2: 948–961
195 Yan D, Zhang H, Xu D, et al. Numerical study of compact terahertz gas laser based on photonic crystal fiber cavity. J Lightwave Technol, 2016, 34: 3373–3378